Old Dominion University
ODU Digital Commons

Electrical & Computer Engineering Theses & Dissertations

Electrical & Computer Engineering

Summer 1992

# A Novel Technique for Deep Level Characterization of High-Resistivity Semiconductor Materials

Sridhar Panigrahi
*Old Dominion University*

Follow this and additional works at: https://digitalcommons.odu.edu/ece_etds

Part of the Electronic Devices and Semiconductor Manufacturing Commons, and the Semiconductor and Optical Materials Commons

## Recommended Citation

Panigrahi, Sridhar. "A Novel Technique for Deep Level Characterization of High-Resistivity Semiconductor Materials" (1992). Master of Science (MS), Thesis, Electrical & Computer Engineering, Old Dominion University, DOI: 10.25777/k36c-2189
https://digitalcommons.odu.edu/ece_etds/465

This Thesis is brought to you for free and open access by the Electrical & Computer Engineering at ODU Digital Commons. It has been accepted for inclusion in Electrical & Computer Engineering Theses & Dissertations by an authorized administrator of ODU Digital Commons. For more information, please contact digitalcommons@odu.edu.

# A NOVEL TECHNIQUE FOR DEEP LEVEL CHARACTERIZATION OF HIGH-RESISTIVITY SEMICONDUCTOR MATERIALS

by

Sridhar Panigrahi
B. Sc. in Electrical Engineering, May 1977
Sambalpur University, India

A Thesis Submitted to the Faculty of
Old Dominion University in Partial Fulfillment of the
Requirements for the Degree of

MASTER OF SCIENCE

ELECTRICAL ENGINEERING

with an emphasis in Physical Electronics

OLD DOMINION UNIVERSITY
August, 1992

Approved by:

---

Dr. V. K. Lakdawala (Director)

---

Linda L. Vahala

---

Hasan Erkaya

ABSTRACT

A NOVEL TECHNIQUE FOR DEEP LEVEL CHARACTERIZATION OF HIGH-RESISTIVITY SEMICONDUCTOR MATERIALS

**Sridhar Panigrahi**

**Old Dominion University**

**Director: Dr. Vishnu. K. Lakdawala**

An improved photo induced current transient spectroscopy (PICTS) technique is developed for studying deep level parameters in high-resistivity semiconductor materials. A new digital data acquisition approach and improvement in the cryogenics of the system have enabled us, for the first time in our laboratory, to detect $Cu_A$ level in a copper doped silicon compensated gallium arsenide (GaAs:Si:Cu) sample. The digital approach improves both the signal to noise ratio (S/N) and the efficiency of the system. Also, multiple PICTS spectra in a single thermal cycle can be obtained. In the present work, various doped and undoped gallium arsenide (GaAs) and polycrystalline zinc selenide (ZnSe) crystals are studied. The current transients are analyzed by using two different methods -- a standard rate window method and a curve fitting method. The relative merits and demerits of the two methods are discussed. It has been observed that multiple decay time constants obtained from the curve fitting method consist of sum of the exponentials throughout the temperature range centered around the resonant peak. In particular, this method allows the separation of closely spaced traps within the bandgap.

## ACKNOWLEDGEMENTS

It is my privilege to thank Dr. Vishnu K. Lakdawala for his guidance and support throughout my research work. I would like to thank Dr. Hasan Erkaya and Dr. Linda L. Vahala for their valuable comments in this manuscript and being in my committee. My special thanks to Dr. Karl H. Schoenbach, Dr. Ralf Peter Brinkmann for numerous discussions which significantly improved the experimental methodology and analysis of my work. I am thankful to Lucy M. Thomas and Gordhan R. Barevadia for various discussions on the research work. I deeply appreciate the help extended to me by Raymond Allen and Benny Stokes during hardware and software simulation of the experiment. The courtesy extended by John Kenney, Raymond Allen, Sabine Ludwig, and Benny Stokes was invaluable and is deeply appreciated. My utmost gratitude and appreciation are for the graciousness of my brother's family for their longstanding encouragement throughout this program.

# TABLE OF CONTENTS

Page

**ACKNOWLEDGEMENTS** . . . . . . . . . . . . . . . . . . . . . . . . . . . . . . . . . . . . ii

**TABLE OF CONTENTS** . . . . . . . . . . . . . . . . . . . . . . . . . . . . . . . . . . . . iii

**LIST OF TABLES** . . . . . . . . . . . . . . . . . . . . . . . . . . . . . . . . . . . . . . v

**LIST OF FIGURES** . . . . . . . . . . . . . . . . . . . . . . . . . . . . . . . . . . . . . vi

**LIST OF SYMBOLS** . . . . . . . . . . . . . . . . . . . . . . . . . . . . . . . . . . . . viii

Chapter

1. **INTRODUCTION** . . . . . . . . . . . . . . . . . . . . . . . . . . . . . . . . . 1

   Electronic transitions and trapping effect . . . . . . . . . . . . . . . . . 4
   Review of previous work . . . . . . . . . . . . . . . . . . . . . . . . . . . 9
   Organization . . . . . . . . . . . . . . . . . . . . . . . . . . . . . . . . . . 12

2. **THEORY OF PHOTO INDUCED CURRENT TRANSIENT SPECTROSCOPY** . . . . . . . . . . . . . . . . . . . . . . . . . . . . . . . . 14

   Rate window method . . . . . . . . . . . . . . . . . . . . . . . . . . . . . 15
   Curve fitting method . . . . . . . . . . . . . . . . . . . . . . . . . . . . . 19

3. **SYSTEM MODIFICATION** . . . . . . . . . . . . . . . . . . . . . . . . . . 23

   Cryogenic cell modification . . . . . . . . . . . . . . . . . . . . . . . . . 25
   Digital approach to data acquisition . . . . . . . . . . . . . . . . . . . 28

4. **SAMPLE PREPARATION AND TESTING** . . . . . . . . . . . . . . . . . 34

   Mounting arrangement of samples . . . . . . . . . . . . . . . . . . . . . 34
   Sample testing . . . . . . . . . . . . . . . . . . . . . . . . . . . . . . . . 40

5. ANALYSIS OF EXPERIMENTAL RESULTS AND DISCUSSIONS . . . . . 41

Analysis . . . . . 41
Experimental results . . . . . 45
GaAs:Si:Cu sample . . . . . 45
Polycrystalline ZnSe sample . . . . . 47
SI GaAs sample . . . . . 49
SI GaAs (LEC grown) sample . . . . . 51
SI GaAs (VBT grown) sample . . . . . 55
GaAs:Cr sample . . . . . 58
Discussions . . . . . 58
Sources of error and analysis . . . . . 64
Conclusions . . . . . 67
Scope of future work . . . . . 69

LIST OF REFERENCES . . . . . 71

APPENDICES

Appendix-A . . . . . 76

Appendix-B . . . . . 79

Appendix-C . . . . . 81

Appendix-D . . . . . 95

## LIST OF TABLES

Table Page

1. Specification of various samples used for the characterization studies. . . . . . . . . . . . . . . . . . . . . . . . . . . . . . . . 35

2. Energy level of shallow level traps in different samples. . . . . . . . . . . 44

3. Trap level parameters of semiconductor samples using the rate window method. . . . . . . . . . . . . . . . . . . . . . . . . . . . . . . . . 54

4. Deep level parameters obtained using the curve fitting method. . . . . . . . . . . . . . . . . . . . . . . . . . . . . . . . . . . . 62

5. A comparison of deep level parameters between the rate window method and the curve fitting method. . . . . . . . . . . . . . . 63

## LIST OF FIGURES

Figure | Page


1. Common electronic transitions in photoconductors (a) Absorption and excitation (b) Trapping and capture, (c) recombination. . . . . . . . . . 5

2. Current transient induced by a laser pulse. . . . . . . . . . 16

3. An schematic of previous PICTS set-up for the rate window method. . . . . . . . . . 24

4. A cross-sectional view of the Boss cryogenic cell. . . . . . . . . . 26

5.(a) Schematic of modified arrangement for the PICTS experiment. . . . . . . . . . 29

5.(b) Schematic of experimental arrangement for PICTS on ZnSe. . 32

6. A planar geometry configuration of a sample. . . . . . . . . . 36

7. Mounting arrangement of a sample on TO-18 header. . . . . . 38

8. DC Current-Voltage (I-V) characteristic of samples. (a) GaAs (LEC grown), GaAs(VBT grown),GaAs:Cr.samples. (b) polycrystalline ZnSe. . . . . . . . . . 39

9. The mode parameters versus temperature plot of SI GaAs sample.43

10. (a) A typical PICTS spectrum of the GaAs:Si:Cu sample. (b) An arrhenius plot of GaAs:Si:cu sample using the rate window method. . . . . . . . . . 46

11. (a) A typical PICTS spectrum of polycrystalline ZnSe sample. (b) An arrhenius plot for the peaks of ZnSe sample using the rate window method. . . . . . . . . . 48

12. (a) A typical PICTS spectrum of SI GaAs sample showing EL2 peak.

| | | |
|---|---|---|
| | (b) An arrhenius plot of SI GaAs sample for the EL2 peak obtained using the curve fitting technique. | 50 |
| 13. | (a) A typical PICTS spectrum of GaAs(LEC grown) sample. (b) An arrhenius plot of GaAs(LEC grown) sample obtained using the rate window method. | 52 |
| | (c) An arrhenius plot of SI GaAs(LEC grown) sample using the curve fitting method. | 53 |
| 14. | (a) A typical PICTS spectrum of GaAs(VBT grown) sample. (b) An arrhenius plot of GaAs (VBT grown) sample obtained using the rate window method. | 56 |
| | (c) An arrhenius plot of GaAs (VBT grown) sample using the curve fitting method. | 57 |
| 15. | (a) A typical PICTS spectrum of Cr-doped GaAs sample. (b) An arrhenius plot of GaAs:Cr sample obtained using the rate window method. | 59 |
| | (c) An arrhenius plot of GaAs:Cr sample obtained using the curve fitting method. | 60 |
| C.1 | Confidence intervals in 1 and 2 dimensions. | 86 |
| C.2 | Confidence region ellipses corresponding to values of chi-square larger than the fitted minimum. | 86 |
| C.3 | Energy level diagram of GaAs:Si:Cu at 300K. | 88 |

## LIST OF SYMBOLS

| Symbol | |
|---|---|
| $a_k$ | adjustable parameter of $k^{th}$ point |
| $C_{uA}$ ,$C_{uB}$ | energy levels of copper in gallium arsenide(eV) |
| $C_k$ | constant for $k^{th}$ mode |
| $\chi^2$ | chi-square |
| **D** | matrix function |
| $d^*$ | excited layer thickness |
| $\nabla$ | vector operator |
| $E_a$ | activation energy of trapped electrons or holes |
| $E_c$ | bottom of conduction band |
| $E_v$ | top of the valence band |
| $e_n$ | emission rate of electron from the trap |
| $\gamma_n$ | constant depends on the density of states in the relevant band, temperature, and thermal velocity |
| $h$ | planck's constant |
| I | current (DC) |
| i(t) | transient or instantaneous current |
| $i(t_\infty)$ | dark current |
| j | integer number |

| | |
|---|---|
| K | boltzmann's constant |
| KT | thermal energy |
| L | width of sample |
| l | gap between contacts on the sample |
| l' | length of sample |
| $\lambda_k$ | decay constant of $k^{th}$ mode |
| M | integer number |
| $m^*$ | effective mass of electron or hole |
| $\mu_n$ | mobility of an electron |
| N | number of data points |
| $N_C$ | effective density of states in conduction band |
| $N_{CuA}$ ,$N_{CuB}$ | concentration of copper levels in gallium arsenide |
| n | electron number density |
| $n_t$ | concentration of trapped electron in traps |
| $n_t(t)$ | decay of trapped electron density |
| $n_t(0)$ | initial density of filled electron trap |
| $\nu$ | an integer, known as degree of freedom |
| P | probability function |
| p | number density of holes |

| | |
|---|---|
| $p_t$ | concentration of trapped holes |
| $p_t(t)$ | decay of trapped hole density |
| Q | probability function complement of P |
| q | electronic charge |
| $\sigma_n$ | capture cross-section of an electron |
| $\sigma_i$ | standard deviation of $i^{th}$ point |
| $t_\infty$ | time at infinity |
| $\tau_t$, $\tau_{max}$ | relaxation time of trapped carriers |
| $\tau_n$ | life time of an electron |
| T | absolute temperature in Kelvin |
| $T_m$ | temperature at peak of PICTS spectrum |
| $t_1$,$t_n$ | time in second |
| $v_{th}$ | thermal velocity of an electron or a hole |
| V | voltage or potential |
| $x_i$ | x coordinate of ith point of current transient |
| $y_i$ | y coordinate of ith point of current transient |

# CHAPTER 1

# INTRODUCTION

Compound direct semiconductor materials of group III-V, such as doped and undoped gallium arsenide (GaAs), have found fast growing applications in computing, in fiber optic communications, and as a switch material for pulsed power applications, mainly due to their high electron mobilities and inherent optical properties [1]. Zinc selenide (ZnSe), also a compound direct semiconductor material of group II-VI, has the potential for efficient high power switching in opening and closing mode operation [2]. The DC breakdown voltage of ZnSe is an order of magnitude higher than that of GaAs, thus making it a good candidate for photoconductive switch material [3]. In addition, this material can be used for optoelectronic and photodetector devices. Deep level impurities, which give rise to energy levels within the forbidden gap of semiconductor materials, are important from both the performance and reliability point of view in device fabrication. Sometimes, the semiconductor materials are doped intentionally to create deep levels, to achieve specific device requirements, such as speed of the device, and resistivity of the material. These high resistivity materials are semi-insulating in nature and are used as a substrate material for IC fabrication [4]. For the purpose of modelling and fabrication of these devices, information on the physical

parameters, such as energy level, capture cross-section, and concentration of these trap centers is necessary.

Various characterization techniques, such as photoluminescence (PL), thermally stimulated current (TSC), deep level transient spectroscopy (DLTS), and photo induced current transient spectroscopy (PICTS) have been used to determine the trap parameters. Photoluminescence is not a suitable method to determine trap parameters because impurities involved in non-radiative recombinations are not detected and therefore, detracted from the PL signal. In addition, it is difficult to measure concentration of the impurities by this method [5]. TSC provides limited information, and data interpretation is difficult due to high dark current above room temperature [6]. DLTS is not useful for high resistivity material due to small junction capacitance and difficulties in injecting free carriers with a voltage pulse. PICTS is most suitable for detecting and characterizing deep level impurities in semi-insulating semiconductor material, because this method is suitable for injecting free carriers into high resistivity materials by optical excitation. Basically PICTS consists in the analysis of the thermal behavior of the photocurrent transient induced by a periodic laser pulse. The behavior of the trap centers and electronic transitions within the bandgap of semiconductor material upon optical excitation using a periodic laser pulse is discussed later in this chapter.

PICTS measurement technique has been implemented at the Physical Electronic Research Institute, Old Dominion University, to characterize high resistive semiconductor switch materials used for pulsed power application [7]. The present

work is an extension of the earlier work, wherein a modified data acquisition system has been developed. This modified (digital) approach is efficient, has an improved signal to noise ratio (S/N), and is capable of generating and acquiring multiple PICTS spectra in a single thermal cycle. In addition, a novel curve fitting technique has been developed to analyze the current transients using an algorithm developed by *Brinkmann* [8] [Appendix-D]. This technique can separate out closely spaced traps, which could not be achieved using the standard rate window method.

The samples characterized in the present work are all semi-insulating in nature. Of the six samples, three GaAs samples are received from Lawrence Livermore National Laboratory (LLNL) for characterization. GaAs samples grown by different techniques are studied using both the rate window technique and the curve fitting technique to study the deep level distribution, if any. The curve fitting technique could separate out closely spaced trap levels within the bandgap which is not possible using the rate window technique. Improvements in the cryogenics of the PICTS system allowed us to successfully detect for the first time $Cu_A$ level (see Appendix-C, Fig. C.3) in silicon doped copper compensated GaAs (GaAs:Si:Cu) sample in our laboratory. A second modified PICTS system has been implemented to characterize high bandgap (2.67 eV at 300K) ZnSe material in this study.

*ELECTRONIC TRANSITIONS AND TRAPPING EFFECT*

The energy band diagram of a pure semiconductor material can be represented by a valence band and a conduction band separated by the bandgap. This bandgap is called a forbidden gap, since an electron cannot occupy any energy level within this zone. Discrete energy levels are introduced into the bandgap during crystal growth, due to either foreign atoms or defects. Such levels are known as generation-recombination (G-R) centers or traps. G-R centers which lie in the bandgap ($\geq$ 3KT below conduction band) are known as deep energy level impurities or, simply, deep-level impurities. The deep level impurities are commonly metallic impurities like iron, gold, chromium, and copper. Deep level impurities are also the result of crystal imperfections, such as dislocations, stacking faults, vacancies or interstitials. Sometimes they are intentionally introduced to alter device properties. In GaAs, deep level impurities raise the substrate resistivity creating semi-insulating substrate. Besides this, the switching time of a device is also reduced by introducing a controlled amount of deep-level impurities.

The electronic transition phenomena in semiconductors with application of a periodic laser or light source changes the conductivity property of the material. These transitions are classified into three categories: (1) absorption and excitation, (2) trapping and capture, and (3) recombination [Fig. 1]. A detailed discussion of these transitions can be found in standard text books [9]. However, a brief

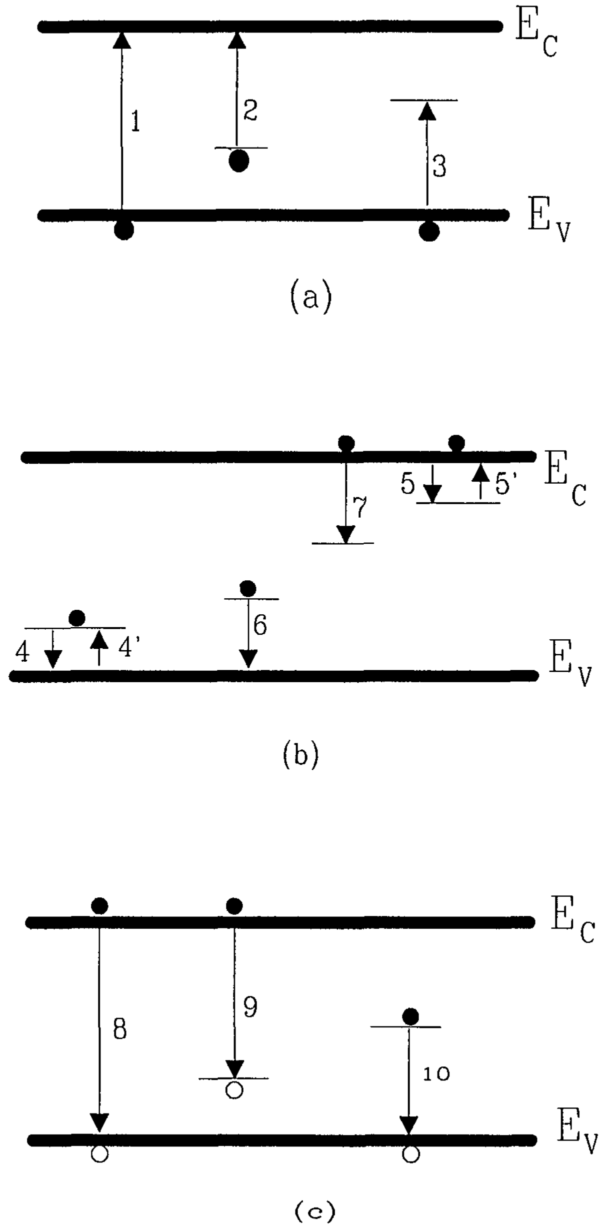


Fig. 1 Common electronic transitions in photoconductors (a) absorption and excitation, (b) trapping and capture, (c) recombination.

description of these transitions relevant to the present work is given below for completeness.

Absorption and Excitation:

Fig. 1(a) shows three types of absorption transitions which result in photoconductivity. Transition 1 corresponds to absorption of optical energy by the atoms of the crystal, producing a free electron-hole pair. Transition 2 corresponds to absorption at defect center in the crystal producing a free electron and bound hole near the defect center. Transition 3 corresponds to absorption, raising an electron from the valence band to an unoccupied defect center producing a free hole and a bound electron near the defect center. The band diagram of Fig. 1(a) indicates that certain minimum energy is required for these transitions and this minimum energy corresponds to the bandgap for transition 1. The wavelength of photon energy corresponding to the bandgap is called the absorption edge. For the light of energy greater than the minimum required absorption is continuous and fairly constant depending on the density of states in the conduction band ($E_C$). Therefore, photoconductivity depends on the wavelength of the exciting laser or the light source.

Trapping and Capture

Fig. 1(b) shows the trapping and capture phenomena in a semiconductor. Once electrons and holes have been freed by absorption of a photon of sufficient energy, they will remain free until they are captured at defect centers. The capturing centers may be classified in two groups: (1) trapping centers, if the captured carrier has a greater probability of being thermally re-excited to the free state than

recombining with a carrier of opposite nature at the defect center, and (2) recombination centers, if the captured carrier has a greater probability of recombining with a carrier of opposite nature at the defect center than of being re-excited to the free state. Fig. 1(b) shows trapping and thermal release phenomena of electrons in the electron trap (transition 5 and 5'), trapping and thermal release of holes in hole traps (electron transition 4 and 4'); also the capture of an electron (transition 7) and of a hole (electron transition 6) in the recombination centers. Although a center with an energy level lying near one of the band edges will be more likely to act as a trap than a recombination center, the distinction between traps and recombination centers is distinguished on the basis of the relative probability of thermal ejection versus recombination. A recombination center may act as a trap at different light levels and temperature.

Recombination

Fig. 1(c) shows the recombination transitions. The free electron combines directly with the free hole (transition 8). Recombination may also occur through recombination centers. An electron may be captured by an excited hole (transition 9), or a hole may be captured by an excited center containing an electron (transition 10).

It is important to clearly distinguish between these transitions when attempting to interpret photo induced current transients, as will be discussed later in chapter 4. Deep energy levels seem to be present in all known semiconductors. In the case of an ideal semiconductor (no energy levels in a forbidden gap), it may be true that

every excited carrier in the crystal would be a free carrier. If a material existed with only recombination centers, in which the majority carrier lifetime is much greater than the minority carrier lifetime, then it would be true that every excited carrier would be a free carrier. If, however, as is the case in almost all real semiconductor materials, there are trapping centers, and the number of free carriers may be less than the number of excited carriers.

A major effect of trapping is to make the decay time of the photocurrent, after excitation has ceased, longer than the carrier lifetime. If no trapping centers are present, then the photocurrent will decay in the same way as the density of free carriers, and the decay time will be equal to the carrier lifetime. If the trapping centers are present, but the free-carrier density is much greater than the density of trapped carriers, again the decay time of the photocurrent will be equal to the carrier lifetime. But, if the density of free carriers is comparable to or less than the density of trapped carriers, the thermal release of trapped carriers during the course of the decay can prolong the decay so that the decay time is longer than the recombination time of the free carriers. Therefore, if the trapped carrier density is greater than the free carrier density, then the decay of photocurrent is effectively dominated by the rate of trap emptying rather than by the rate of recombination. This phenomena generally occurs when a semiconductor sample is irradiated with a periodic laser or light pulse and forms the basis of the PICTS technique.

*REVIEW OF PREVIOUS WORK*

A brief review of recent work on PICTS current transient analysis by other researchers is presented in the following. To accurately accomplish the photo induced current transient analysis, it is important to perform a curve fitting process. The curve fitting analysis, which is based on the principle of transients composed of a sum of exponentials with different decay time constants that can be fitted to obtain a best fit, is proposed as a reliable method to determine trap parameters.

Brasil *et al.* [10] have used a curve fitting method, using a successive substraction procedure on the current transients to compute decay time constants or deep level parameters. They have shown that the current transients obtained from SI GaAs using PICTS can be uniquely fitted by a sum of exponentials. The assumption of a single exponential transient, made in an analysis of the rate window technique can, therefore, lead to a sizable error. The researchers indicate that the fitting procedure may be used along with the PICTS spectrum obtained using the conventional rate window method. The PICTS spectrum is useful for qualitative determination of traps present in the semiconductor and can be used in association with the fitting procedure. In this work, the researchers have reported that EL2 level, which is considered as a dominant deep center in SI GaAs, is, however, seldom observed by PICTS measurement. In addition, the authors observed a large difference between the results obtained using rate window method and curve fitting method. In particular, the trap cross-sections obtained by two-gated rate window

method are larger than those obtained using the curve fitting method. They conclude that the characterization of high-resistivity material is a relatively difficult task and the PICTS technique appears to be the most useful tool currently available to obtain information about deep level traps in SI materials.

Abele *et al.* [11] have employed a digital approach for data acquisition and attempted to find the form of the non-exponential decay. The successive subtraction procedure was employed to evaluate decay constants, and the process was continued until the number of remaining data points are sufficient for reliable determination of amplitude and decay constant. Relying on the sum of three or four exponentials to explain the data was problematic for two reasons. First, the larger the number of parameters used to fit a particular curve, the less reliable the fit. By using eight parameters (amplitude and time constant for four exponentials), one should be able to fit almost any wave form. However, the eight parameters are not independent. The particular set of exponential parameters chosen to fit a particular curve was not necessarily unique. Local minima may exist in the standard error so that another parameter set may give an equally good fit. The authors have suggested that to overcome the problem associated with the successive subtraction procedure, the data can be analyzed in such a way that the exponents are stored simultaneously. One method of doing this is known as method of moments. Using approximate starting parameters (amplitude and time constants) for these exponentials, they used a Newton-Raphson iteration technique to adjust the parameters, so that the moments calculated from them coincide with the data moments. When the fit satisfactorily

converges, the errors in the exponential parameters involved are quite small -- typically a few parts per million in the amplitudes and less than a percent in time constants. In their opinion, the number of exponentials are solved simultaneously, rather than successively.

A similar curve fitting procedure using the least square method was applied to current transients to compute trap parameters or decay constants by Hlinomaz *et al.* [6]. Their work is based on the comparison of results obtained from PICTS measurement on SI GaAs by using a boxcar integrator and the curve fitting procedure. TSC measurement was restricted below room temperature to avoid the influence of dominant dark current. The curve fitting of transients at low temperature range (160K to 190K) could separate out a number of trap levels greater than those observed in using boxcar integrator. Above room temperature, the transient fitting provides close to the same result as the PICTS spectrum. A possible explanation of these observations can be the superposition of the charge emissions from several closely spaced levels which leads to the creation of one broad peak in the PICTS spectrum. In addition, the researchers observed that in many cases the energy level obtained using transient fitting is larger than the PICTS measurement using a boxcar integrator. They have demonstrated that the curve fitting of transients provides more real information in comparison with the rate window technique due to independent evaluation of the whole transient. However, the direct transient measurement made by moving the boxcar gate is very time-consuming.

A detailed discussion on the characterization of GaAs material using the PICTS system available at ODU has been described in an earlier thesis [7]. The current transients obtained using PICTS were analyzed employing the two-gated rate window method. The system had low temperature limitation (upto 128K) and, therefore, could not detect the $Cu_A$ level (required temperature 93K) in the GaAs:Si:Cu sample. However, for the ongoing research on this switch material, it is important to know the physical parameters, such as energy level, capture cross-section, and concentration, of the $Cu_A$ level, because the turn-on performance of the bulk optically controlled semiconductor switch (BOSS) (developed by *Schoenbach et al.* [12] at Old Dominion University) depends on the partition ratio of copper ($N_{CuB} / N_{CuA}$) [12,13]. In addition, the result of modelling studies has revealed that the curve fitting diagnostic technique can separate out closely spaced trap levels within the bandgap which could not be separated out by using the two-gated rate window method. In this work the existing system is improved and a novel curve fitting diagnostic technique for data analysis has been developed in order to address some of the problems encountered in the earlier system.

## *ORGANIZATION*

The theory of PICTS applied to both the rate window method and the curve fitting method, used for transient analysis is discussed in Chapter 2. PICTS system modifications accomplished to improve characterization technique are discussed in

Chapter 3. In Chapter 4 the sample preparation and current-voltage (I-V) characteristic to verify the resistivity of the semiconductor samples are discussed. Finally Chapter 5 presents the analysis of experimental results, discussions, sources of error and analysis, scope of future work and conclusions.

# CHAPTER 2

# THEORY OF PHOTO INDUCED CURRENT TRANSIENT SPECTROSCOPY

The photo induced current transient spectroscopy is employed to measure the deep level parameters of SI GaAs and ZnSe because this method is suitable for injecting free carriers into high resistivity materials. Besides this, a small heat treatment (around 200 $^0$C for 20 minutes) which prevents existing deep level redistribution in the crystal is required for contact deposition on the sample [14]. In the modeling studies the PICTS signal is defined under a physical assumption when one type of dominant trap and several fast recombination centers are present in the sample [15]. However, the experimental conditions are more complex. One of the simplest causes which may influence the standard PICTS spectra is the non-constant pre-exponential factor in the current transients. In such a case, two main methods of analysis in the PICTS measurements have been proposed. In the first method, the rate window concept is applied to current transients stimulated by thermal emission after periodic laser irradiation. The corresponding PICTS peaks with a linear increase in the amplitude with respect to emission rate can be observed when the mobility and lifetime of carriers are independent of temperature. However, the nature of the trap (electron or hole) cannot be distinguished from the PICTS spectrum because both types give a PICTS signal of the same polarity. In the second

method, we have assumed that thermally stimulated current transient consists of a sum of exponentials with decay time constants that can be uniquely determined by the curve fitting method. Each decay constant represents a trap level. The trap parameters obtained from the second method seems to be more reliable than those obtained from the conventional two-gated rate window method. The theories of both methods are described below.

### *RATE WINDOW METHOD*

A typical photo-current transient of SI GaAs is shown in Fig. 2. It is assumed that the current transient is due to one type of trap (electron or hole). The initial current (part AB of the transient) represents the generation of photo-carriers (electron and hole pair) due to band edge excitation (> 1.42 eV at 300K) of GaAs by the irradiating monochromatic laser pulse. During part BC, it is observed that the current transient slowly rises to saturation, which illustrates that, carriers are trapped by the traps (filling of traps). Part CD is related to the steady state photo-current when all the traps are filled up (saturation state). However, the initial amplitude of the current transient is proportional to the total concentration of traps ($N_T$), to the emission rate and constant recombination lifetime $\tau_n(t_\infty)$. When the laser pulse is turned off, the current drops (portion DE of the transient), an activity which represents the recombination of the photo-carriers. This phenomenon occurs rapidly and depends on the recombination lifetime of the free carriers. In the case of a

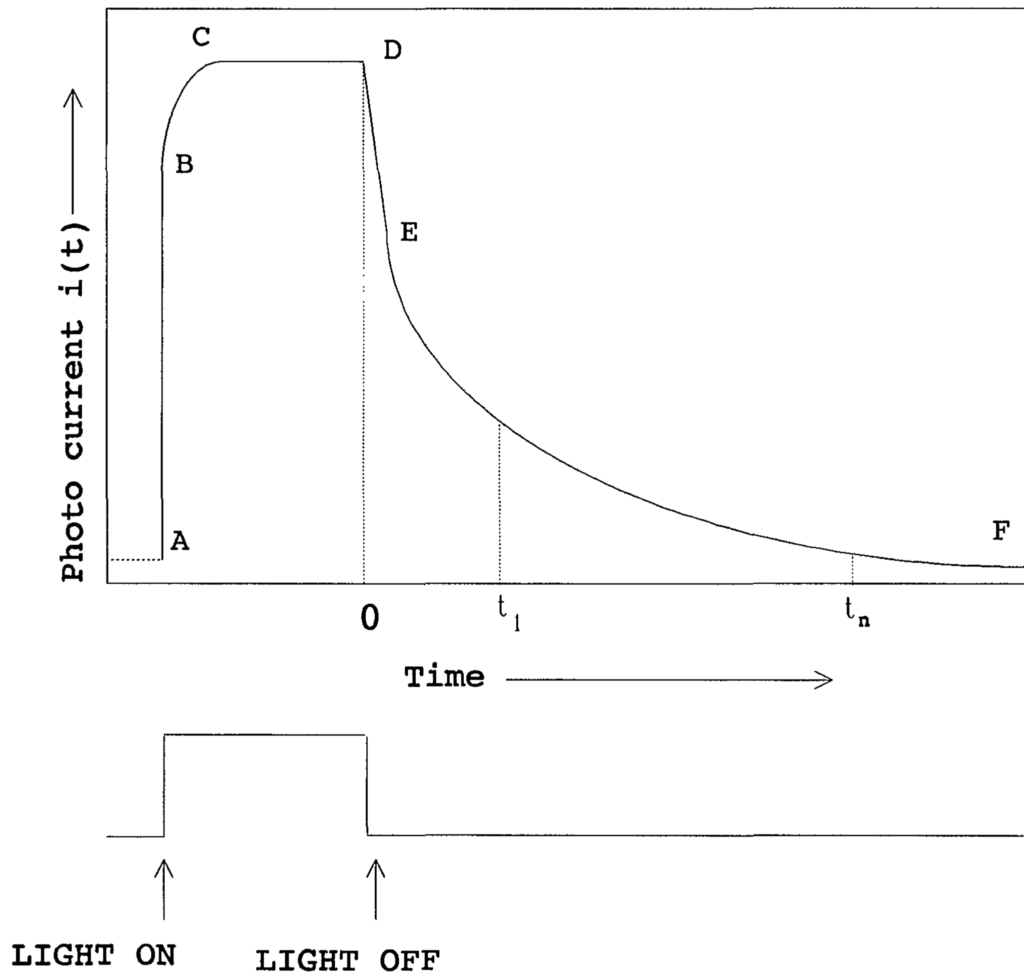


Fig. 2 A typical current transient induced by a laser pulse.

typical GaAs semiconductor, the recombination lifetime of photo-carriers is generally of the order of nanoseconds. Part EF of the current transient represents the thermally stimulated carriers generated from the traps within the bandgap of a semiconductor material. This phenomenon occurs due to the inherent physical properties of a semiconductor to be able to return to its equilibrium condition. This part (EF) of the current transient is mainly of interest in investigating deep level parameters. It is assumed that the duration of the laser turn-off is long enough that the traps are empty at point F ($t=t_\infty$). The current at F is thus assumed to be the dark current of the sample.

We assume that, all the traps are filled at point D of the transient and therefore, the rate of change of carriers with respect to time at that point ($t=0$) is zero. This can be represented by the following equations,

$$\left(\frac{dp}{dt}\right)_{t=0} = 0 \ , \qquad \left(\frac{dn}{dt}\right)_{t=0} = 0 \tag{2.1}$$

$$\left(\frac{dp_t}{dt}\right)_{t=0} = 0 \ , \quad \left(\frac{dn_t}{dt}\right)_{t=0} = 0 \tag{2.2}$$

where, p, n, $p_t$, and $n_t$ are the concentration of free holes, free electrons, and trapped holes and trapped electrons, respectively. The period of darkness is assumed to be long enough so that the traps are empty at point F ($t=t_\infty$). The trapped carriers at point F of the transient can be represented by the following equation,

$$p_t(t_\infty) = 0 \ , \qquad n_t(t_\infty) = 0 \tag{2.3}$$

where $p_t(t)$ and $n_t(t)$ represent the decay of trapped hole and electron density, respectively, at the trap. This is possible because we have assumed that a number of density of states are available for each trap level. If retrapping during the dark period is negligible, then it can be assumed that current transient is an exponential function of time. Then, the electron current due to the emission of traps can be represented by the following equation,

$$i(t) = \mu_n \tau_n \, q \, \frac{L}{l} \, d^* \, v \, n_t(0) \, \frac{1}{\tau_t} \exp\left(-\frac{t}{\tau_t}\right) + i\,(t_\infty) \tag{2.4}$$

where, $\tau_t$ is known as the relaxation time and is related to the parameter of the electron trap, $\mu_n$ and $\tau_n$ are the mobility and lifetime of free electrons, and $n_t(0)$ is the initial density of filled traps (assumed electron traps). Also, $d^*$ is the excited layer thickness. The relaxation time $\tau_t$ is related to the trap depth $E_a$ (with respect to valence band) and capture cross section $\sigma_n$ by the following expression,

$$\frac{1}{\tau_t} = e_n = \sigma_n \, v_{th} \, N_c \exp\left(-\frac{E_a}{KT}\right) \tag{2.5}$$

where $e_n$ is the emission rate of electron from the traps, $v_{th}$ is the thermal velocity of electrons, $N_c$ is the effective density of states, and $E_a$ is the activation energy of trapped electrons. Each of these terms can be expressed as follows.

$$v_{th} = \left(\frac{3KT}{m^*}\right)^{\frac{1}{2}} \tag{2.6}$$

$$N_c = 2\left(\frac{2\pi m^{*}KT}{h^2}\right)^{\frac{3}{2}} \tag{2.7}$$

$$N_c\, v_{th} = \gamma_n\, T^2 \tag{2.8}$$

Therefore, equation (2.5) can be expressed as follows:

$$\frac{1}{\tau_n} = e_p = \sigma_n \gamma_n T^2 \exp\left(-\frac{E_a}{KT}\right) \tag{2.9}$$

In the rate window technique **i(T) = i($t_1$) - i($t_{n}$)** , where i(T) is transient current as a function of temperature. Generally, $t_n$ is very large with respect to $t_1$ ($t_n > 10\, t_1$), then i(T) goes through maximum at the temperature $T_m$ where the condition $\tau_t(T_m)=\tau_m=t_1$ is satisfied [16]. A plot of **ln ($T_{max}^2\, \tau_m$)** against **($1/T_{max}$)**, known as an arrhenius plot, is obtained using equation 2.5, and is used to determine trap parameters.

## *CURVE FITTING METHOD*

This method involves analysis of current transients which are fitted by a sum of exponentials. A curve fitting algorithm developed by Brinkmann R.P. is employed to determine the decay constants corresponding to each exponential. It has already been reported by other researchers that in the case of SI GaAs, the current transient can be uniquely fitted with the sum of exponentials [17].

Fig. 2 represents a typical current transient of a semiconductor sample. The decay generally represents three regions such as (i) a rapid decay region for $t < 1$ms, (ii) a slow decay region for $t > 90$ ms, and (iii) an intermediate decay region in between 1ms and 90 ms.

The rapid decay region of the transient represents the photo-carrier recombination. It has been reported that this region is due to the release of carriers from traps with high emission constants at the measurement temperature [10]. The slow region of the current transient corresponds to carriers released by traps having small capture cross-section at that temperature. Due to dark current intensity, decay constants obtained from this slow decay region will not provide reliable information on trap depth. Therefore, reliable values can be obtained when the intermediate region of transients is fitted with exponentials. The number of points of the transient to be fitted are adjusted to obtain a best fit.

The current transient after laser irradiation can be represented by the following relation,

$$i(t) = \sum_k C_k \lambda_k \exp\left(-\lambda_k t\right) \tag{2.10}$$

where $C_k$ and $\lambda_k$ are termed amplitude and decay constants respectively. The parameter $\lambda$ is equal to $(\tau_t)^{-1}$ , where $\tau_t$ is the trap relaxation time. In the above equation, $k$ represents the number of exponents (*modes*), obtained by curve fitting on the transient and each mode corresponds to one deep level.

The program performs a least square fit on the selected region of the current transient starting with one mode and subsequently more. This minimization proceeds

iteratively. After each step a statistical analysis is performed, based on a chi-square test, to analyze whether the improvement in the sum of the square deviation is significant or not [18-21]. With nonlinear dependence, the minimization proceeds iteratively. This can be represented by the following relation.

$$\chi^2 = \sum_k \left( i_k - C_k\lambda_k \exp(-\lambda_k t) \right)^2 \tag{2.11}$$

During testing, the program adjusts the parameters so that actual data fit the expected data. The more the degrees of freedom, the better the fit [21]. However, only if it is considerably better, is it significant. If an improved fit turns out not to be significant, the one before will be displayed as the *"conservative estimate."* The decay constants corresponding to the various trap levels are subsequently determined. The deep level parameters are then computed from the arrhenius plot as described earlier.

The adjustable parameters, amplitude ($C_k$) and decay time constant ($\lambda_k$) of each mode are used to obtain a best fit of a transient (ref. eqn. 2-10). The program, first selects a set of $C_k$ and $\lambda_k$ and curve fit the transient. If this fit is not good, the program then chooses a second set of those parameters along with the first set, to fit the transient. The goodness-of-fit is realized by the program such that, if the value of decay time constant ($\lambda$) fails to decrease by a factor of ten, then the MRQMIN routine (Appendix-C) is called repeatedly until a convergence is achieved. In the second set, the number of parameters are to be fitted are four and they are interdependent. This procedure continues, until a best fit is obtained. If the number of fitted parameters increases, then the computation becomes complex. After a best

fit is obtained, the program plots the statistical confirmed parameter set, showing different modes, and their possible deviation from the mean value. This plot is of the form of ellipsoids and their boundaries represents the chi-square boundaries as the confidence limits [Appendix-C, Fig. C.1 and C.2]. The smaller the ellipse, the better the fit is.

The following chapter describes the system modification accomplished to achieve accurate and reliable acquisition of data for the PICTS experiment.

# CHAPTER 3

# SYSTEM MODIFICATION

A schematic of the earlier PICTS set-up used to characterize various semiconductor samples is shown in Fig. 3. Section A of the Fig. 3 shows the cryogenic cell (cryostat), and section B represents the electronics of the system necessary for acquiring data. A CW He-Ne laser and an adjustable shutter was used to irradiate the sample with a pulsed laser beam to generate current transients. The lowest temperature achieved in the system was 128K (-145$^0$C). This temperature is not low enough to detect the $Cu_A$ level in the GaAs:Si:Cu sample. Besides using this setup, the experiment had to be repeated at least four to five times to generate multiple PICTS spectra, which are required for trap parameters calculation. Also, the current transients were digitized into a small number of data points (512), they hence provided poorer resolution. Thus, to overcome these limitation and to improve the efficiency of the PICTS experimental system, modifications ( particularly in the sections A and B ) were necessary.

Basically the system modification has been implemented in two areas: (i) in the cryogenic cell (section-A) to reduce the cold finger temperature capability up to 77K (-196$^0$C), (ii) the data acquisition system to generate multiple PICTS spectra and increase the number of digitized data points per transient. Apart from this, the

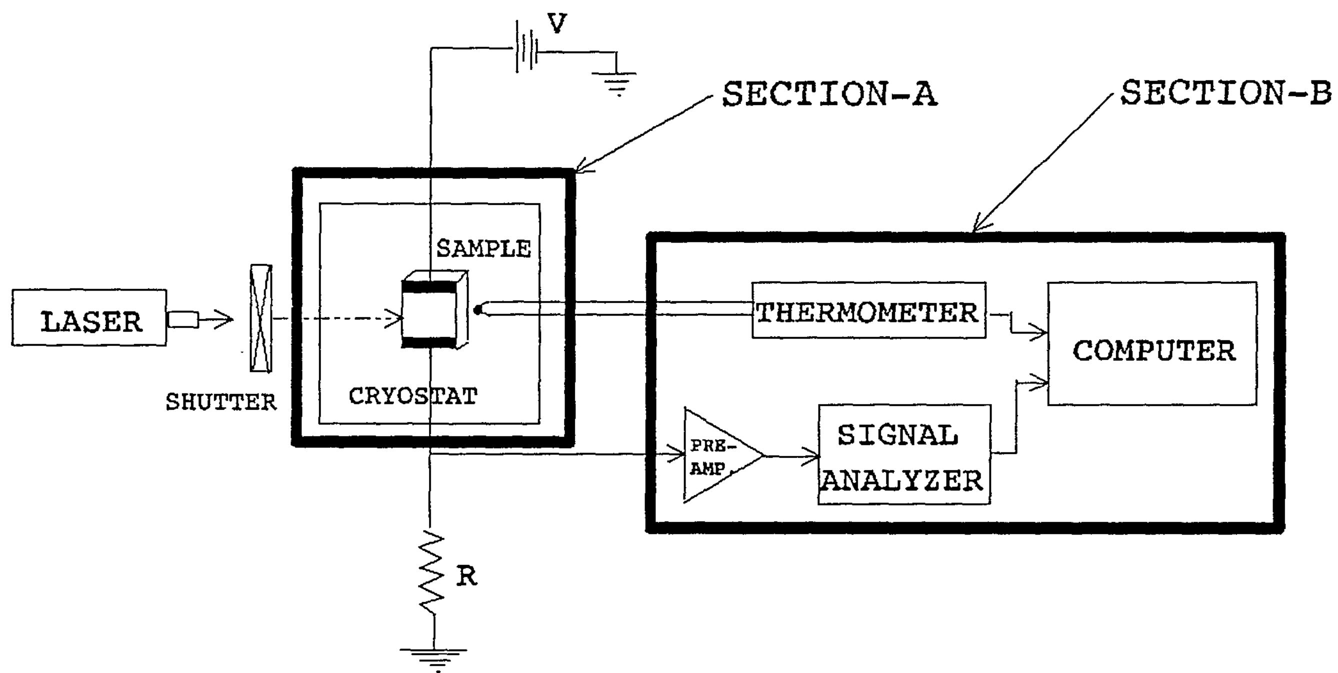


Fig. 3 A schematic of previous PICTS set-up for the rate window method.

system is also modified to characterize high bandgap material such as, ZnSe (2.67 eV at 300K) [22]. The details of these modifications accomplished are described below.

*CRYOGENIC CELL MODIFICATION*

The photo induced current transient spectroscopy (PICTS) technique employed to characterize deep level parameters of semi-insulating (SI) semiconductors was being conducted in a liquid nitrogen cooled cast aluminum metal cryostat. A lowest temperature of 128K was achieved in the system, a level which is not low enough to determine the $Cu_A$ level in a GaAs:Si:Cu sample. Detection of this level is very important for the proper understanding of the BOSS switch currently being developed at ODU [12]. This optically controlled switch can be turned ON as well as OFF, on command with a laser light pulse at two different wavelengths [12]. Cu forms deep acceptor levels in GaAs, and the influence of copper deep levels ($Cu_A$ and $Cu_B$) plays an important role in the switch performance. The higher the $N_{CuB}/N_{CuA}$ ratio, the shorter the switch opening time [23]. Also, the recent results show that partition is small ($N_{CuA}$ large) when the copper diffusion process takes place under no arsenic over pressure [13]. Thus, knowledge of $N_{CuA}$ and $N_{CuB}$ is very useful to develop appropriate switch manufacturing technique.

A new cryostat known as **BOSS CRYOGENIC CELL** (Fig. 4) is designed and fabricated in association with Tetra Corporation using stainless steel as the material for the cell body. The cold finger of the cell is designed with brass due to its high

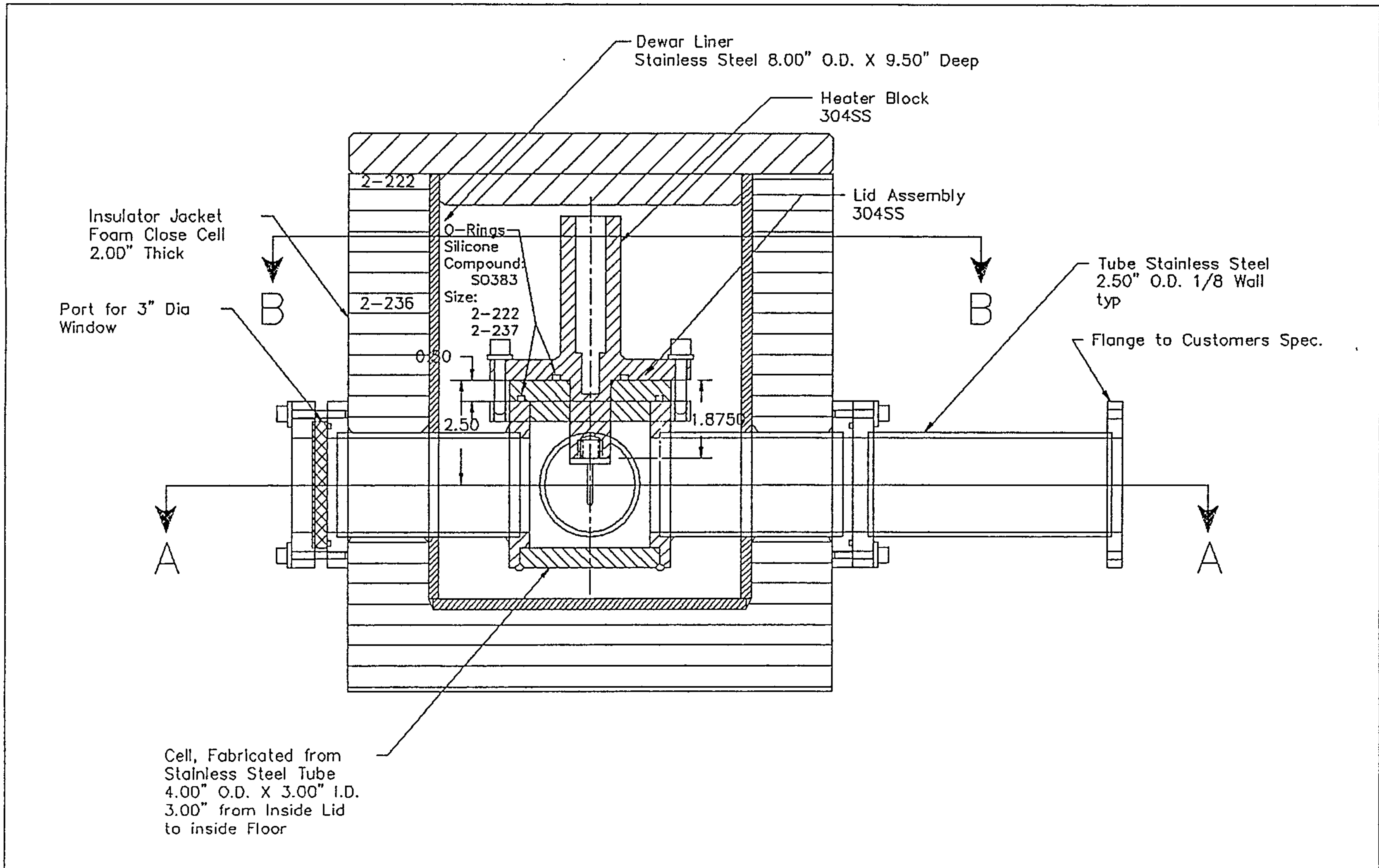


Fig. 4 A cross-sectional view of the Boss Cryogenic Cell.

thermal conductivity property. The cryogenic cell is then thermally insulated from the ambient using styrofoam around the body. The cell has four openings (windows) diametrically opposite around the body. One opening is used to tap signal output from the sample and the thermo-couple. The second port is connected to the vacuum pump for evacuating the chamber, and the third port, which is opposite to this vacuum port, is used as the view port for the inner cell and has a glass (quartz) window. The fourth port has a quartz glass window to allow the laser beam to pass through it to be incident on the sample. It is important to know that for the laser beam to pass through the (quartz glass) window, the energy of the beam must be less than the band edge excitation of quartz glass which is the case in our experiments. This port protrudes outside, in order to avoid frost deposition on the glass during the cooling cycle of the experiment. The top of the cell can be removed to insert the sample into the inner chamber. All the ports are sealed with silicone O-rings of different sizes to keep the inner cell vacuum tight. The cell is kept under vacuum using a roughing pump to achieve a low temperature within a minimum time. In addition, creating a vacuum inside the cell is essential because this prevents water condensation on the sample and the quartz window during the cooling cycle. The system takes about an hour and half to achieve temperature as low as 84K. The $Cu_A$ level at 0.14 eV activation energy could be successfully detected using this new cryogenic cell (temperature around 93K).

*DIGITAL APPROACH TO DATA ACQUISITION*

The system set-up is modified to study photo induced current transient spectroscopy of semiconductor materials based on a digital signal averaging technique. This digital approach solves some of the problems encountered in the previous system (section B of Fig. 3). A schematic of the modified arrangement for the PICTS experiment is shown in Fig. 5(a). The system can be divided into four sections such as the temperature control system, the optical system, the electronic and data recording system, and a stable d.c. power supply source. Both temperature and data recording systems have been significantly modified from the earlier arrangement. Each of the sub-systems is described in some detail below.

The sample is mounted on the cold finger of the cryogenic cell and the temperature is varied from 84K up to 400K using either liquid nitrogen or a manually controlled electric heater. A precision temperature scanner (Keithley meter) is used to display and digitize temperature data up to two decimal points of resolution. The temperature can be controlled and acquired up to a 0.2 $^0$C variation. An OMEGA make T-type temperature sensor (copper-constantan thermo-couple) is embedded in the cold finger to transduce the correct temperature signal of the sample into a voltage signal.

The optical system consists of a CW He-Ne laser (5 mW, 6328 Å), Vincent's Uniblitz LS2 electronic shutter driver and an electro-mechanical shutter, and a quartz window which is transparent to the He-Ne laser beam. The electro-mechanical

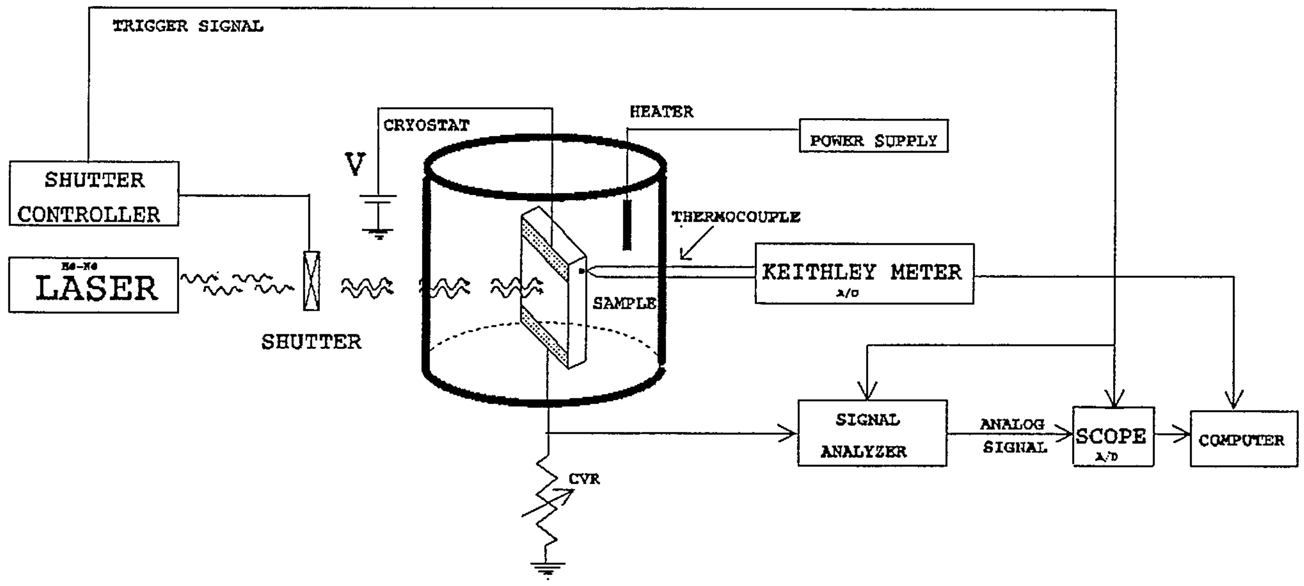


Fig. 5(a) A schematic of modified arrangement for the PICTS experiment.

shutter frequency can be varied electronically from 0 Hz to 400 Hz by the adjustable shutter driver.

The electronic and data recording system for the current signal consists of current viewing resistors, a signal analyzer, a digital storage oscilloscope(Tektronix 2232), and a computer. The signal output from the sample is connected to a current viewing resistor (CVR) which converts the current signal into a voltage signal. The output signal is very small and therefore, needs amplification for further processing. Hence, the output of the CVR is connected to a signal analyzer which serves two purposes -- first, it amplifies the signal amplitude ten times; secondly, it restores the base line of the transient which otherwise can change due to the temperature dependent dc signal (dark current). This change in dc level is continuously subtracted from the current transients by the analyzer. As a result, the base line of the signal remains in a fixed position on the oscilloscope throughout the temperature range during the experiment. The baseline correction is an important requirement during the experiment.

A low d.c. bias voltage obtained from a steady d.c. source is applied to one end of the sample, and the other end is connected to the CVR. A low electric field is required in these experiments to keep the electric field dependent current in the linear region.

The storage oscilloscope (scope) receives a signal from the signal analyzer wherein the transients are averaged and digitized. About 32 signals are averaged to obtain an improved signal to noise ratio. This averaged transient is digitized

(sampled) to 1024 points equally spaced in time with a 8-bit resolution. These digitized data are transferred to the computer periodically, and the data transfer is controlled by a real time computer program. The transfer of data from the scope, to the computer, which is controlled by the program is possible only when a predetermined change of temperature condition (entered interactively) is satisfied. In our case, data are transferred from the scope to the computer with a preset temperature variation of $0.5^0$C. However, it can be further reduced to $0.2^0$C, for our cryogenic system to obtain a smooth ( closely spaced data points ) spectrum. The only difficulty is that such a large disk space (of about 40K byte) is required for each set of the experiment compared to 15K byte for $0.5^0$C. A GPIB board has been installed in the computer to interface the Keithley thermometer for the temperature signal. The program acquires the temperature signal from the Keithley meter simultaneously and periodically along with the current transient data and stores it in a data file. The stored data are then used to develop the PICTS spectrum and subsequently run the curve fitting program.

For the second part, the system is modified to characterize the high bandgap material (ZnSe with a bandgap of 2.67 eV at 300K). Here a pulsed nitrogen ($N_2$) laser of 3371 Å wavelength (ultraviolet range) with an average power output of 100mW is used for exciting the sample. An experimental setup of PICTS for ZnSe material is shown in Fig. 5(b). The pulse repetition rate of the Nitrogen laser can be varied continuously from 1 to 100 pps. In our experiment, the single-shot pulse

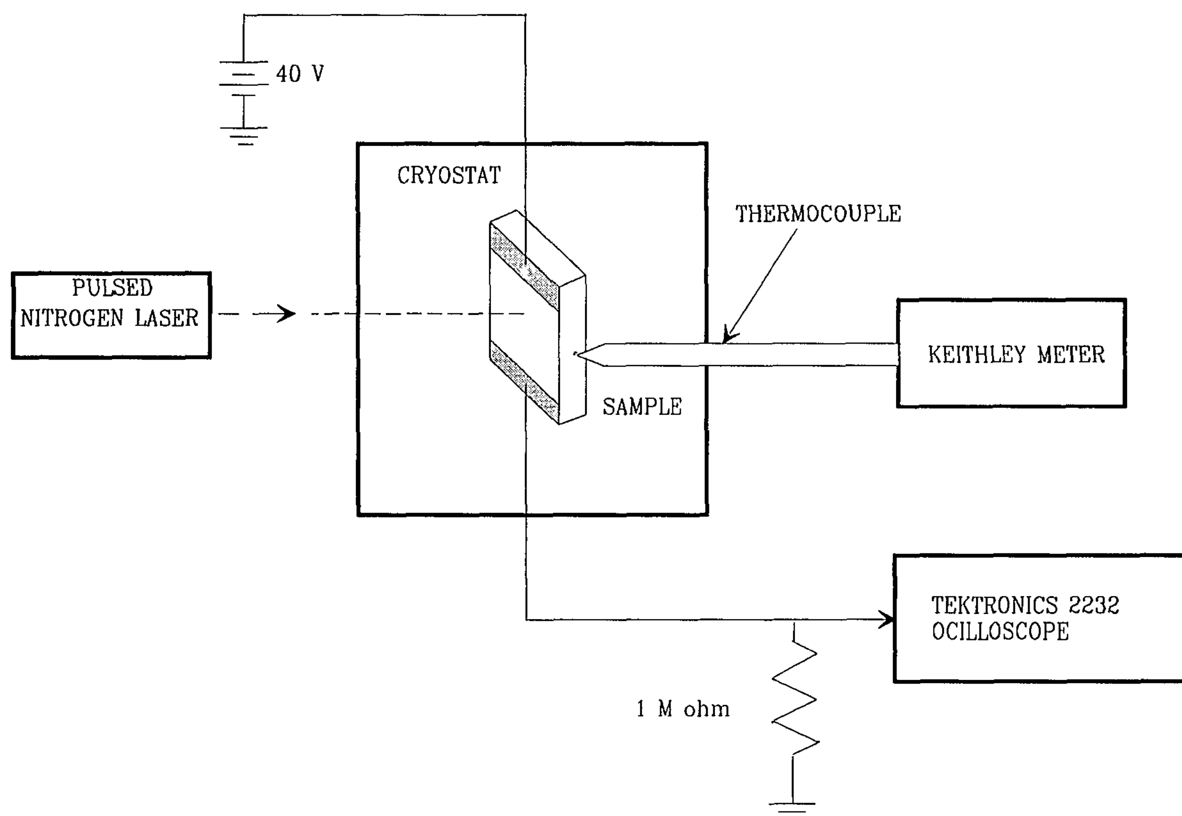


Fig. 5(b) A schematic of experimental arrangement for PICTS on ZnSe.

is manually triggered to generate current transients, which are stored in the storage oscilloscope with a degree rise in temperature.

This digital approach of data acquisition has solved some of the problems encountered earlier in the analog approach. The major advantages of the digital approach is the collection of data in one thermal cycle of the experiment. In an analog approach it is necessary to repeat the experiment for each rate window in order to generate the PICTS spectrum. As a result, the experimental condition may not be the same for the set of experiments introducing inaccuracy in analysis. The dark current can vary an order of magnitude at the same temperature after repeated thermal cycles [11]. Moreover, the electrical properties of contacts may also vary significantly. Second advantage of the digital approach is that the data acquisition is possible with a temperature variation of 0.2 $^{0}$C. The signal can be averaged and digitized as long as it is necessary to reduce the signal to noise level (S/N) ratio. There is a provision to vary the number of transients to be averaged in the oscilloscope. In our experiment thirty-two transients are averaged and stored. The number of transients being averaged is only limited by the capability of the system to maintain a stable temperature and data transfer time. The digital approach is therefore much more efficient and economical compared to the analog approach, since the trap parameters can be extracted from the experimental data in a single thermal cycle.

# CHAPTER 4

# SAMPLE PREPARATION AND TESTING

Sample preparation and testing are vital, from the point of view of device characterization to achieve accurate experimental results. Although samples to be studied are developed with metallization (contacts), they need some processing steps, such as, mounting arrangement, electrical connections to the terminal and testing prior to the PICTS measurement. Specifications of these samples are shown in Table1. This chapter describes, briefly, the nature of the contact, sample configuration, the electrical connection for signal output, and the DC current-voltage (I-V) characteristics of those samples.

## *MOUNTING ARRANGEMENT OF SAMPLES*

A planar geometry configuration of the sample has been used for the PICTS measurement so that the laser beam can shine perpendicularly on the surface of the sample. Ohmic contacts ( Fig. 6) have been developed on one polished surface to connect the sample with a system device because this type of contact has linear or quasi-linear current-voltage characteristics, and voltage drop across the ohmic contact is minimal compared to the drop across the active region of the device. These ohmic

Table 1. Specification of various samples used for the characterization studies.

| **Sample type** | **Dimension (mm) (L x l'x d)** | **Length of Exposed Surface (mm) l** | **Resistivity (ohm-cm)** | **Manufacturer** |
|---|---|---|---|---|
| GaAs:Si:Cu | 2x5x0.76 | 2.0 | $10^5$ | Bertram Lab. Processed at ODU. |
| Poly-crystalline ZnSe | 3x7x1 | 1 | $>10^9$ | Univ. of Maryland |
| Undoped SI GaAs | 1.75x6x0.58 | 1.5 | $7.4 \times 10^7$ | Processed at ODU |
| Undoped SI GaAs (LEC) <100> | 3.9x4.5x2 | 2.2 | $>10^7$ | Showa Denko (Japan) |
| Undoped GaAs (VBT) | 3.9x3.9x1 | 2.6 | $10^9$ | LLNL |
| Cr doped SI GaAs <100> | 3.8x4.8x3 | 2.1 | $>10^9$ | Furukawa (Japan) |

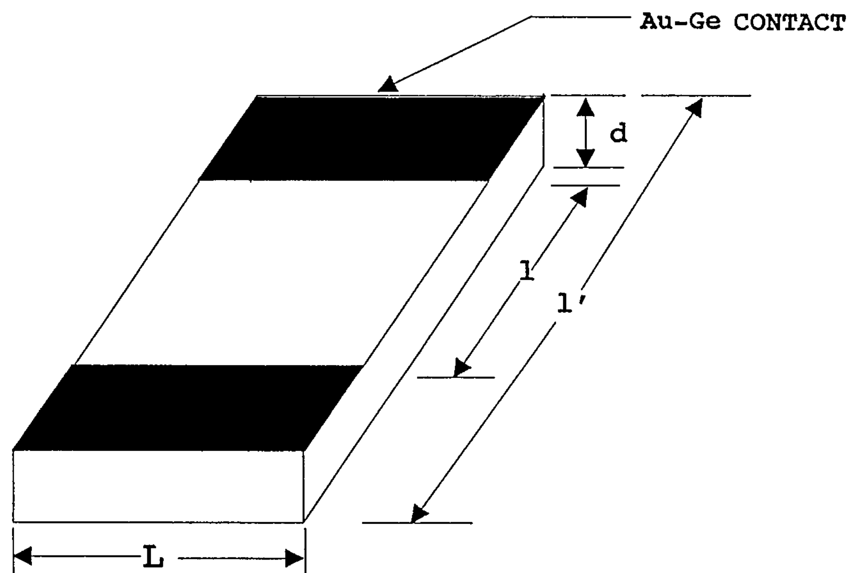


Fig. 6 A planar geometry configuration of a sample

contacts should not inject minority carriers into the device, which may cause measurement error. It has been reported that gold-germanium (AuGe) alloy is suitable to use as an ohmic contact for n-type GaAs and ZnSe semiconductors because this alloy (Au: 88%, Ge: 12%) offers the least potential barrier with the semiconductor, and voltage drop is minimum at the junction [15]. When a metal comes in contact with a semiconductor, electrons and holes move in opposite directions until fermi levels of both materials align. This charge transfer builds up a space charge at the junction, and, as a result, a potential barrier is formed. An ohmic contact should not have this potential barrier at the interface. In practice, a contact is considered ohmic if the voltage drop across the junction is much smaller than across the device. The samples are then mounted on a TO-18 header as shown in Fig. 7. To keep the sample firmly in position and electrically insulated, OMEGABOND-200, a black two-part epoxy is applied on the top of the metallic TO-18 header. Besides being a good electrical insulator, this epoxy is a good thermal conductor and, therefore, capable of making good thermal contact with the metallic header. The sample is then kept inside an electric oven for two hours at an elevated temperature of 204 $^0$C to cure the epoxy. Two tiny pieces of metallic wires are used to connect the sample with the header terminals for electrical connection to the output device. Silver epoxy, a good adhesive as well as a good electrical conductor, is applied to keep wires firmly in position. To cure the silver epoxy, the samples are kept inside an electric oven, around 200 $^0$C for 20 minutes. The samples are then ready for testing.

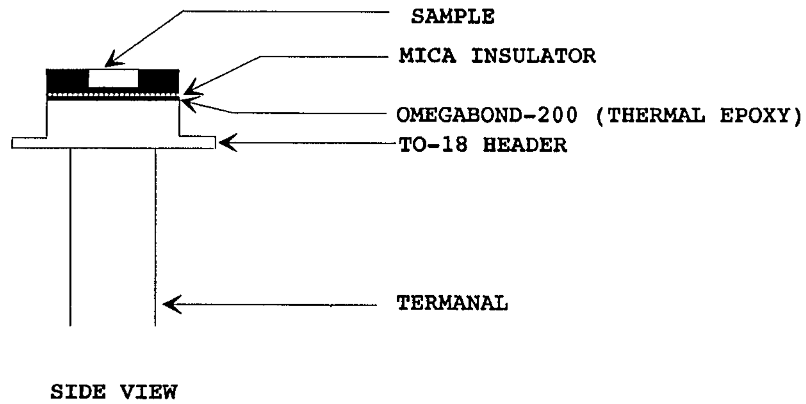


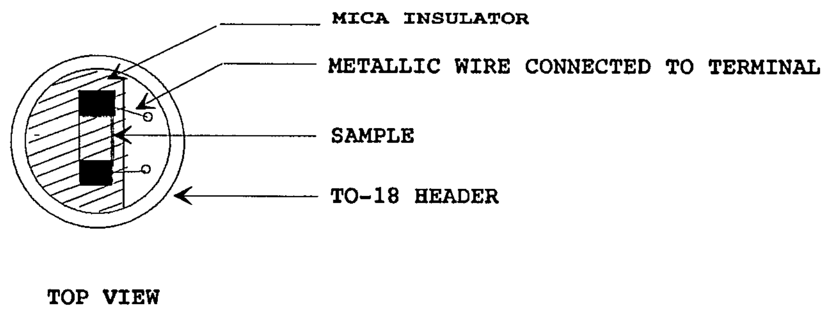


Fig. 7 Mounting arrangement of a sample on TO-18 header.

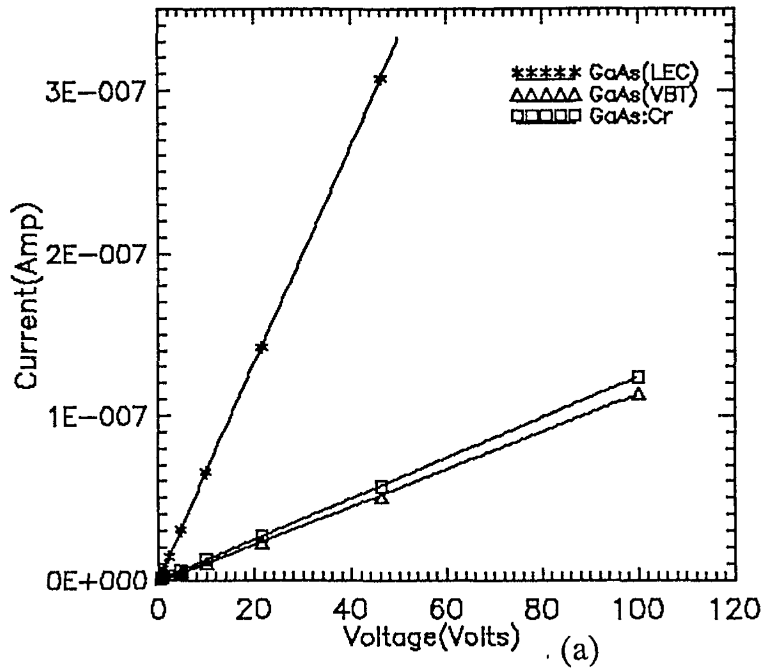


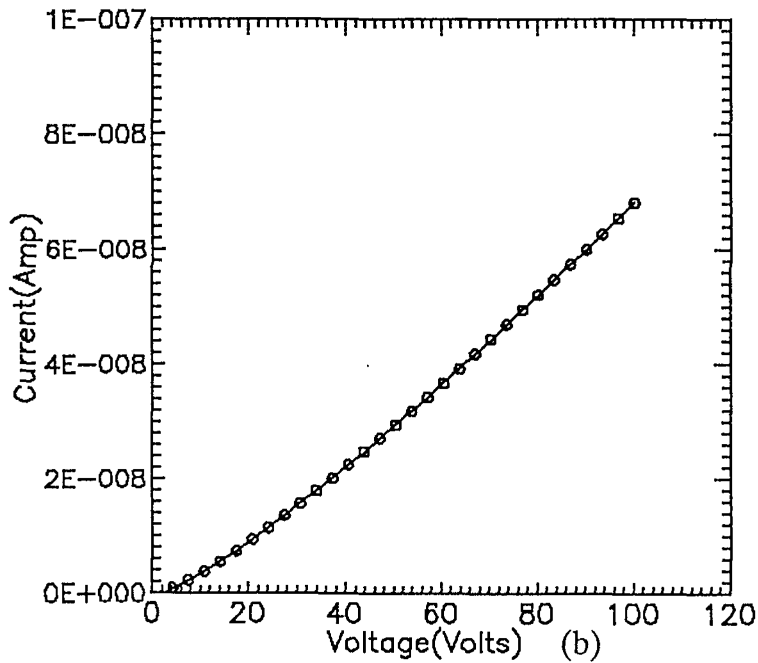


Fig. 8 DC Current-Voltage (I-V) characteristics of samples.
(a) GaAs(LEC grown), GaAs(VBT grown), GaAs:Cr.
(b) poly crystalline ZnSe.

*SAMPLE TESTING*

The sample resistivity and contact characteristics are some of the important parameters of semiconductor samples required to be determined prior to the PICTS characterization. The D.C. I-V characteristics of the samples are taken to establish those parameters. The I-V plots of GaAs (LEC grown), GaAs (VBT grown), GaAs:Cr and polycrystalline samples are shown in Fig. 8(a) and Fig. 8(b) respectively. Clearly, the linear I-V relationship over the measurement range of the electric field indicates that contacts are ohmic in nature. The sample resistivity computed from these plots is greater than $10^7$ ohm-cm, which implies that they are semi-insulating in nature [24]. The resistivity of GaAs:Si:Cu ($10^5\Omega$-cm) and SI GaAs ($> 10^7$ $\Omega$-cm) have been obtained earlier and are shown in Table 1. The above measurements are taken at room temperature (300K). It is observed that the samples are highly resistive in nature. Therefore, the PICTS measurement can be employed with these samples for characterization.

# CHAPTER 5

# ANALYSIS OF EXPERIMENTAL RESULTS AND DISCUSSIONS

This chapter describes the characterization of deep level parameters of GaAs:Si:Cu, ZnSe, SI GaAs, GaAs (LEC grown), GaAs (VBT grown), and GaAs:Cr using two different techniques. Of the six samples, the first two samples, GaAs:Si:Cu and ZnSe (which are used as switch material) are characterized by using the rate-window method. The remaining four samples are characterized using both the rate-window method and the curve fitting method to perform a comparative analysis. In this set the SI GaAs sample was characterized earlier by using the rate-window method in our laboratory [7]. This sample has been chosen for characterization by the curve fitting method because its PICTS spectrum has a very well defined peak at temperature corresponding to the EL2 level and, therefore, served as a calibration sample. An algorithm shown in Appendix-D is used to implement the curve fitting technique for current transient analysis.

## *ANALYSIS*

As discussed in Chapter 2, analysis of transients using curve fitting program provides multiple decay time constants and their corresponding amplitudes (ref.

Appendix-C). These decay time constants (or *modes*) are used to calculate deep level parameters. If we assume that the influence of temperature is minimum (in the equation $(1/\tau_n) = e_p = \sigma_n \gamma_n T^2 \exp(-E_a/KT)$), and the modes are distributed over the entire measurement temperature range, then the plot of $\ln(\lambda)$ against (1000/T) for SI GaAs (slow data acquisition time (ms)) yields shallow levels for these modes as shown in Fig. 9. The other three samples-GaAs (LEC grown), GaAs (VBT grown), and GaAs:Cr also show similar results (Table 2). Also, in earlier work using a fast digitizer (data acquisition time $\mu$s), similar results have been observed [7]. Therefore, for both the fast and slow time scale data acquisition, only shallow levels could be identified using curve fitting for the entire measurement range of temperature compared to both shallow and deep level respectively. This indicates that the assumption made regarding the influence of temperature is not correct because the traps are not electrically active at all temperatures; thus, the idea of traps being active throughout the temperature range cannot be justified. Apart from shallow levels, deep levels are also present in the high-resistivity sample. In view of this, information about the approximate temperature range wherein a peak occurs is extracted from a PICTS spectrum. The current transients close to this temperature range are then considered for evaluation of the decay time constants. Subsequently, these decay time constants are used to determine the activation energy of trap levels. This is logically correct because, in conventional two-gated rate window technique, the temperature ($T_{max}$) corresponding to a peak at different rate-windows is used to calculate trap levels. Since each peak is associated with transients within a

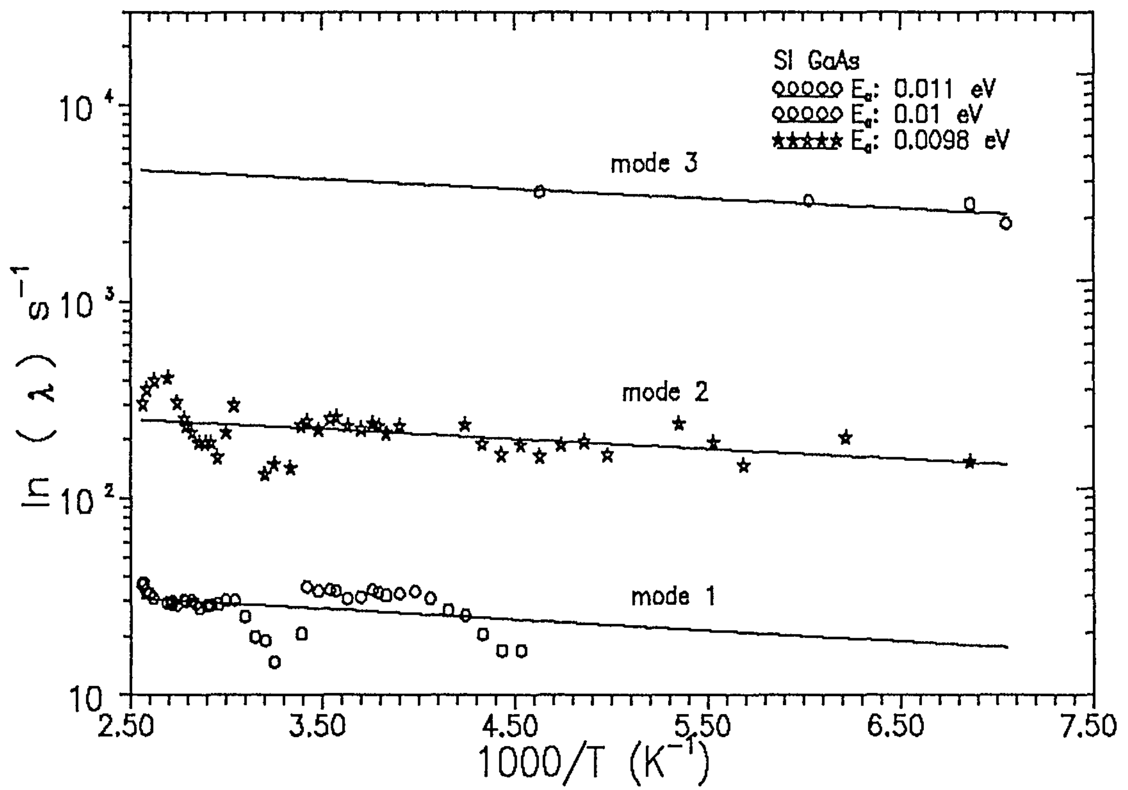


Fig. 9 The mode parameters versus temperature plot of SI GaAs sample.

Table 2. Energy level of shallow level traps in different samples.

| SAMPLE | ACTIVATION ENERGY (eV) |
|---|---|
| SI GaAs | 0.011<br>0.01<br>0.0098 |
| GaAs (LEC) | 0.049<br>0.025 |
| GaAs (VBT) | 0.0013<br>0.0079 |
| GaAs:Cr | 0.008<br>0.012<br>0.0002 |

temperature range, it is therefore, certainly justifiable to consider those transients only for evaluation of trap energy level. These considerations have been applied to evaluate trap parameters using curve fitting technique. When these considerations were complied with, we observed deep levels. A detailed discussion of these results follows.

## *EXPERIMENTAL RESULTS*

### GaAs:Si:Cu sample

A typical PICTS spectrum of copper compensated silicon doped GaAs (GaAs:Si:Cu) obtained from using the rate window method is shown in Fig. 10(a). The spectrum is generated with a rate-window of 56 ms ($t_1$ = 2ms, and $t_n$ = 58ms). The exposure (charging) and decay (discharging) time of laser pulse applied to the sample is 90 ms and 60 ms respectively. Of four peaks, only three, namely pk#1, pk#2, and pk#3, are identified from the spectrum and the corresponding activation energy of those trap levels is 0.14 eV, 0.32 eV, and 0.45 eV respectively. The peak pk#1, which is at 0.14 eV above the valence band, has been detected for the first time in our laboratory experiments and can be tentatively identified as due to $Cu_A$ level [24,25,26,28]. The level at 0.45 eV above the valence band can tentatively be identified as due to $Cu_B$ level [25-28]. The level at 0.32 eV could be due to a $Cu_{Ga}$ $Si_{Ga}$ complex [13]. The energy levels and capture cross-sections are calculated using

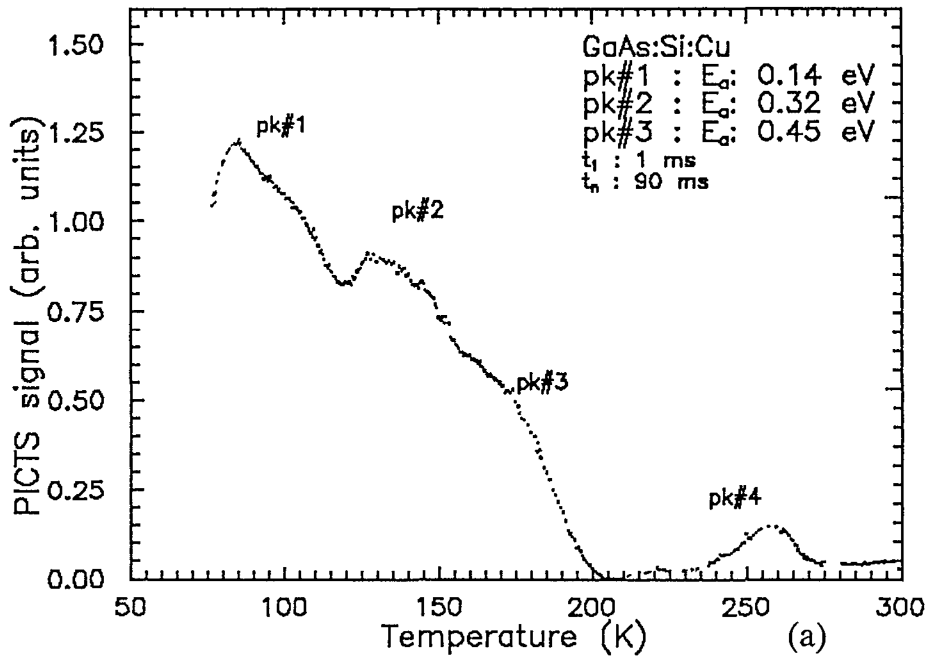


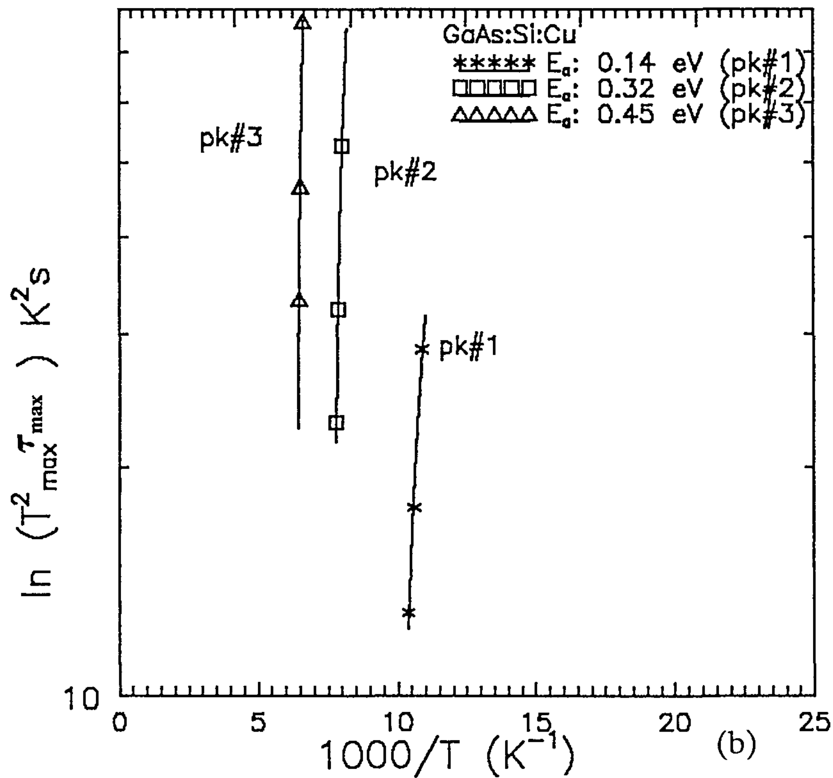


Fig. 10 (a) A typical PICTS spectrum of the GaAs:Si:Cu sample. (b) An arrhenius plot of GaAs:Si:Cu sample using the rate window method.

an arrhenius plot shown in Fig. 10(b). The trap concentrations are calculated from the current transients using equation 2.4. The values of trap parameters are tabulated in Table 3. The capture cross-section is computed using the value of coefficient $\gamma_n$ and $\gamma_p$ $2.3 \times 10^{20}$ $cm^{-2}s^{-1}K^{-2}$ and $1.7 \times 10^{21}$ $cm^{-2}$ $s^{-1}K^{-2}$, respectively [5].

**Polycrystalline ZnSe sample**

A typical PICTS spectrum of polycrystalline ZnSe using the two-gated rate window technique is developed with a window of 1.76 ms ($t_1$=0.04 ms, $t_n$=1.8 ms) and shown in Fig. 11(a). Two peaks, pk#1 and pk#2 around 93K (-180$^0$C) and 153K (-120$^0$C), respectively, are identified in the spectrum. These defects may be due to the selenium vacancy present in the crystal. The trap energy level at 1.03 eV and 0.41 eV associated with peak pk#2 and pk#1, respectively, are extracted from an arrhenius plot shown in Fig. 11(b). The corresponding trap concentrations are of the order of $10^{14}$ $cm^{-3}$. An electron mobility of 900 $cm^2$/V.s and carrier lifetime of 1 ns is considered for calculations of trap parameters. Trap concentrations of this order are also observed by Besomi and Wessely in their study on molecular beam epitaxial grown (MBE grown) ZnSe [30, 31]. However,the exact nature of polycrystalline ZnSe has not been fully investigated and still remains a subject of study.

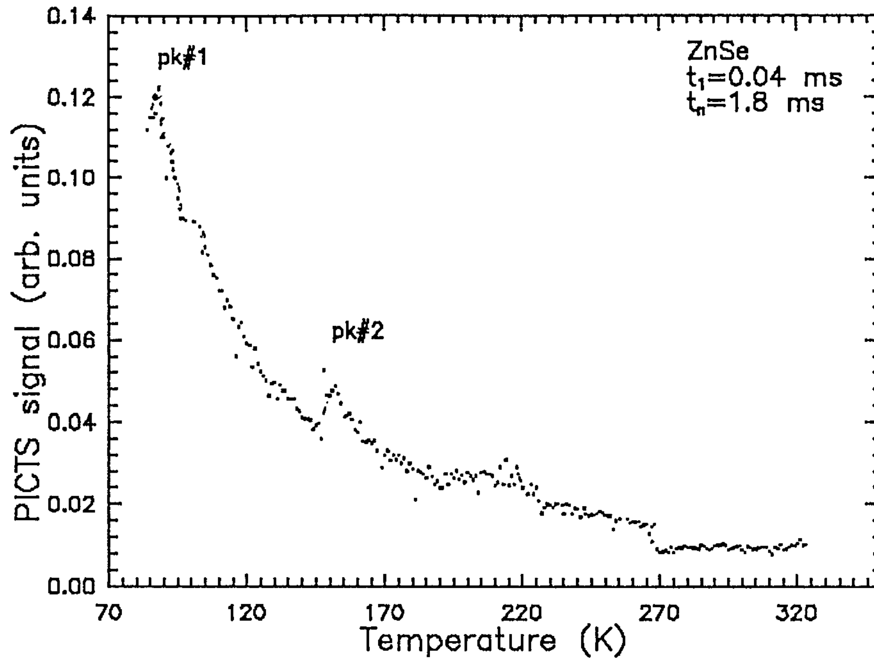


(a)

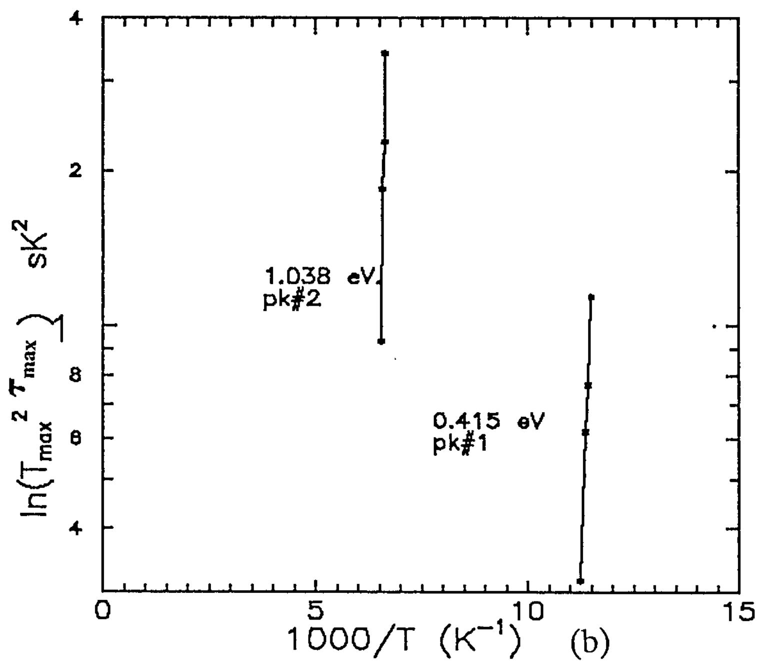


(b)

Fig. 11 (a) A typical PICTS spectrum of polycrystalline ZnSe sample.
(b) An arrhenius plot for the peaks of ZnSe sample using rate window method.

**SI GaAs sample**

This sample was chosen, as a calibration sample, for comparative analysis of two techniques, namely the rate window and the curve fitting technique, because its PICTS spectrum (Fig. 12(a)) has a very well-defined peak with the activation energy of 0.78 eV around 390K [7]. The level at 0.78 eV is assigned as EL2 [15]. Curve fitting analysis is applied to the current transients for this sample within the temperature range of 348K to 393K centered around the peak temperature 390K. Fig. 12(b) indicates the arrhenius plot for this temperature, range and it is observed that three distinct modes at 0.80 eV (mode #1), 0.27 eV (mode #2), and 0.42 eV (mode #3) are separately obtained. The presence of three modes obtained using the curve fitting method indicates that the current transient consists of three time constants in the specified temperature range. The single peak observed in the PICTS spectrum is, therefore, probably a result of three modes. The temperature at which the maximum current emission occurs depends on the activation energy and capture cross-section of the traps (eqn. 2.5). Since these parameters are also a function of temperature, it is conceivable that multiple trap levels can exist for a single peak in the spectrum. This indicates that the curve fitting method which can separate out multiple traps is otherwise not possible by using the two-gated rate window method. The capture cross-section determined by the curve fitting method for the trap (mode #1) is $7.5\times10^{-15}$ $cm^2$, which is in agreement with the results obtained by Brasil *et al.* for this level [10].

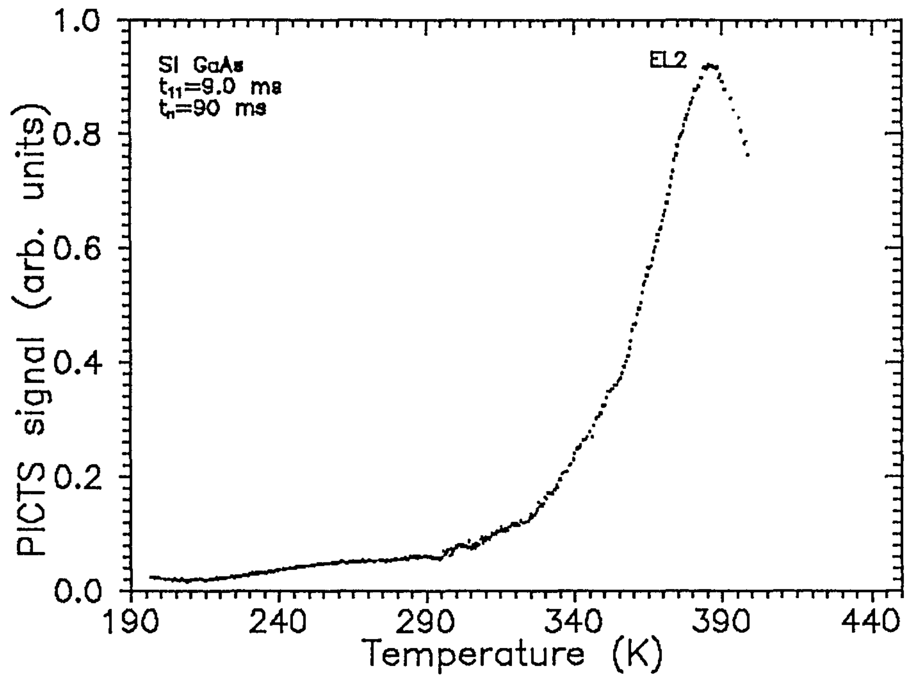


(a)

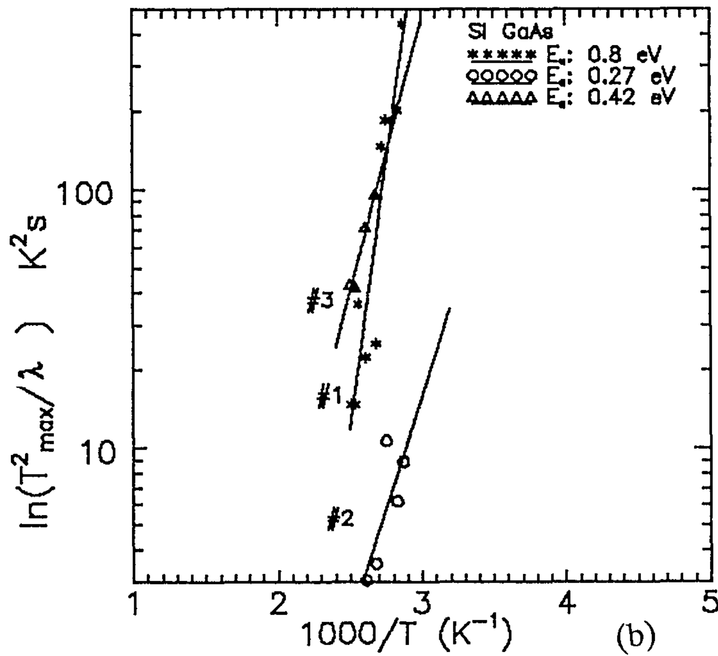


(b)

Fig. 12 (a) A typical PICTS spectrum of SI GaAs showing EL2 peak. (b) An arrhenius plot of SI GaAs sample for the EL2 peak obtained using the curve fitting technique.

**SI GaAs (LEC grown) sample**

A typical PICTS spectrum for a window of $t_1=0.8$ ms and $t_n=90$ ms for SI GaAs (LEC grown) is shown in Fig. 13(a). Four peaks are identified, of which three peaks-such as, pk#2, pk#3, and pk#4 are well resolved. Three trap levels, at 0.85 eV, 0.63eV and 0.21 eV could be identified using the rate-window method. The peak pk#4 at 0.85 eV is in agreement with the trap level designated as EL2 observed by other researchers [32]. The signature of the trap level for peak pk#2 at 0.21 eV is identified as EL17 [14]. The peak pk#3 at 0.63 eV is not identified; however, this level has been observed elsewhere for SI GaAs [10,15]. The curve fitting method is employed to separate out closely spaced trap levels, if any, present in specific temperature ranges. For this purpose, first the PICTS spectrum is referred to in order to identify a certain peak and the corresponding temperature range. Curve fitting is then employed to the transients corresponding to each peak. The energy levels are computed from the arrhenius plot shown in Fig. 13(c). The trap levels obtained from the curve fitting method corresponding to each level obtained by the rate window method are shown in Table 3. The peak pk#4 at 0.85 eV obtained by using the rate window method is resolved into two trap levels such as, 0.66 eV and 0.61 eV by implementing the curve fitting method. Similarly, the peak pk#3 at 0.63 eV is resolved into two levels at 0.57 eV, and 0.55 eV. Different results are obtained for the peak pk#2. It has been reported that trap levels at 0.57 eV, 0.55 eV $(0.56\pm0.01)$ eV and 0.28 eV $(0.27\pm0.01)$ appear in all SI GaAs (LEC grown)

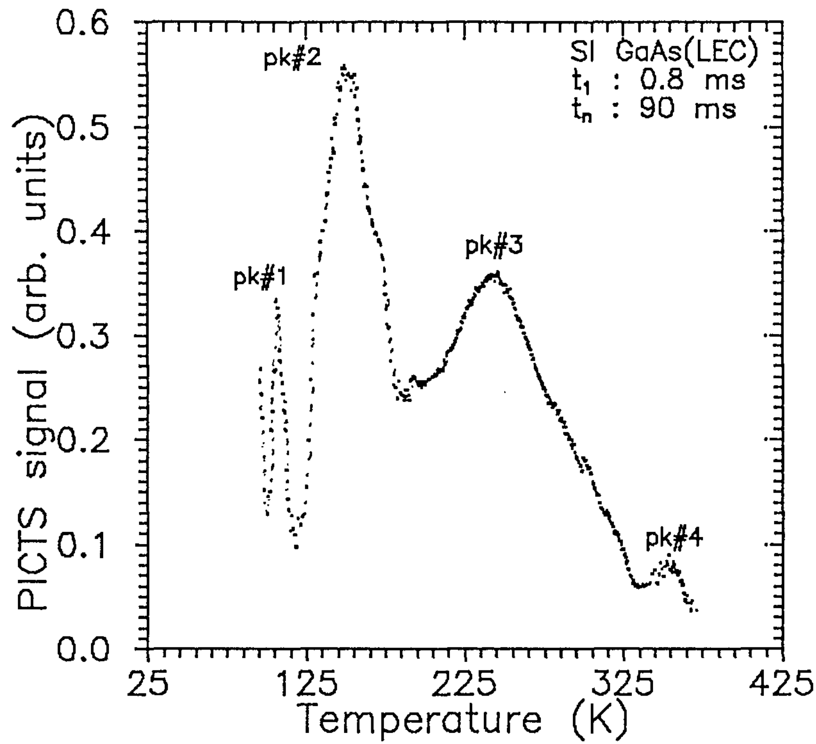


(a)

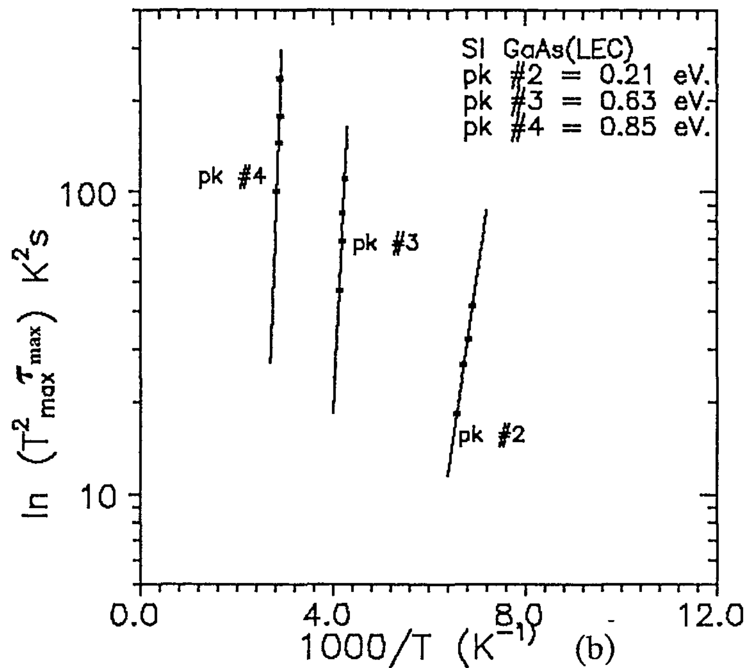


(b)

Fig. 13 (a) A typical PICTS spectrum of GaAs(LEC grown) sample.
(b) An arrhenius plot of GaAs(LEC grown) sample obtained using the rate window method.

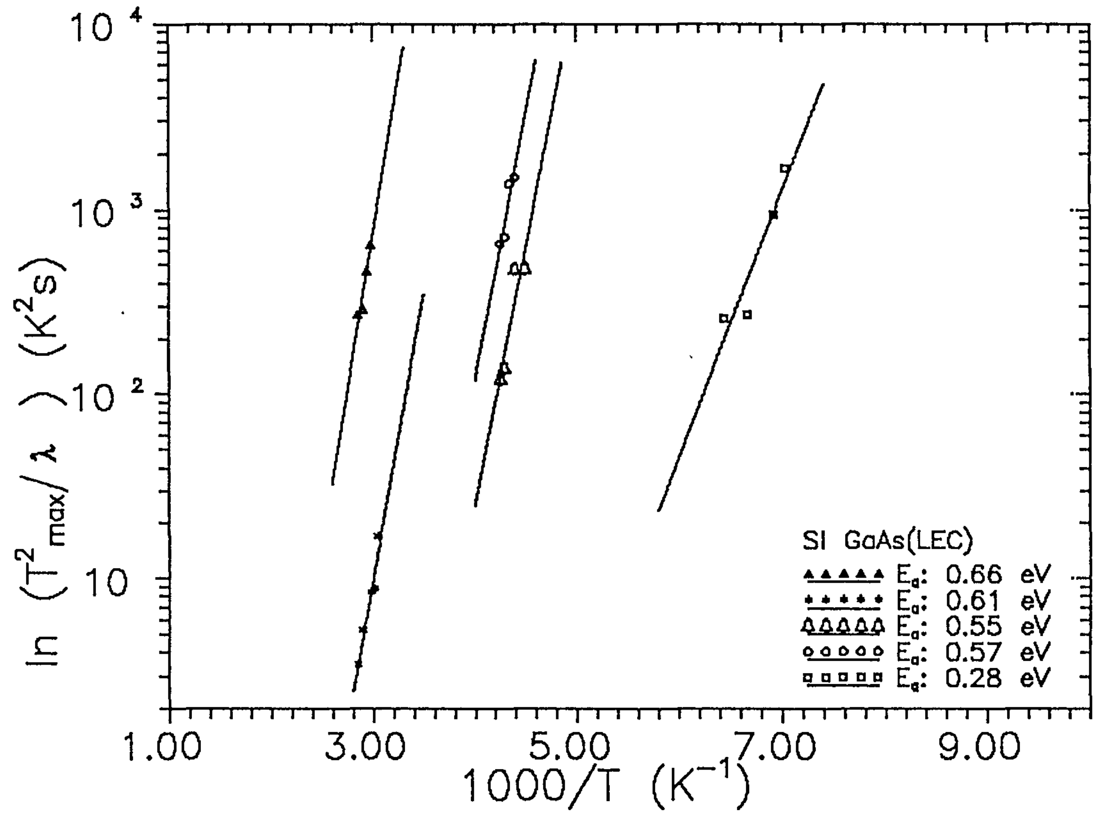


Fig. 13 (c) An arrhenius plot of GaAs(LEC grown) sample obtained using the curve fitting method

Table 3. Trap level parameters of semiconductor samples using the rate window method.

| **Sample** | **Trap Level** | **Activation Energy (eV.)** | **Trap Concentration ($N_T$) $cm^{-3}$** | **Capture Cross-section ($\sigma$) $cm^2$** |
|---|---|---|---|---|
| GaAs:Si:Cu | $Cu_B$ | 0.45 | $2.54 \times 10^{16}$ | $3.0 \times 10^{-10}$ |
| | ? | 0.32 | $5.81 \times 10^{16}$ | $6.0 \times 10^{-11}$ |
| | $Cu_A$ | 0.14 | $9.44 \times 10^{16}$ | $7.0 \times 10^{-16}$ |
| ZnSe | ? | 1.03 | $6.2 \times 10^{14}$ | $4.8 \times 10^{-17}$ |
| | ? | 0.41 | $3.07 \times 10^{14}$ | ? |
| SI GaAs | EL2 | 0.78 | ? | $3.5 \times 10^{-14}$ |
| GaAs (LEC) | EL2 | 0.85 | $1.17 \times 10^{15}$ | $6.09 \times 10^{-10}$ |
| | ? | 0.63 | $4.68 \times 10^{15}$ | $1.05 \times 10^{-9}$ |
| | EL17 | 0.21 | $7.18 \times 10^{15}$ | $3.6 \times 10^{-15}$ |
| GaAs (VBT) | ? | 0.43 | $6.06 \times 10^{11}$ | $1.80 \times 10^{-16}$ |
| | ? | 0.39 | $1.29 \times 10^{12}$ | $1.80 \times 10^{-14}$ |
| | ? | 0.38 | $2.12 \times 10^{12}$ | $6.37 \times 10^{-9}$ |
| GaAs:Cr | EL10 | 0.61 | $1.48 \times 10^{18}$ | $8.54 \times 10^{-15}$ |
| | EL3 | 0.51 | $1.63 \times 10^{18}$ | $4.02 \times 10^{-14}$ |
| | EL12 | 0.16 | $1.17 \times 10^{18}$ | $1.0 \times 10^{-18}$ |

samples, and are attributed to the presence of Fe and Zn impurities. It may be observed that trap levels obtained by both the methods are different. This variation is not unusual. Similar results are also observed by other researchers in their analysis [15]. The reasons for these variations are discussed later in this chapter.

**SI GaAs (VBT grown) sample**

PICTS spectra with different rate windows for GaAs (VBT grown) are shown in Fig. 14(a). The spectra indicates shifts in peak pk#2 with respect to rate window and temperature which is used to obtain arrhenius plot. The spectrum ($t_1 = 1.2$ ms) shows peaks, pk#1, pk#2, and pk#3, within a temperature range of 86.6K through 381K. The corresponding trap levels at 0.38 eV, 0.39 eV, and 0.43 eV are obtained from an arrhenius plot shown in Fig. 14(b). The arrhenius plot of different modes obtained using the curve fitting method is shown in Fig. 14(c) to calculate energy level of modes. We obtained levels corresponding to each mode at 0.2 eV ( for pk#1), 0.32 eV ( for pk#2), and 0.48 eV, 0.3 eV (for pk#3). The level at peak pk#3 is resolved into two trap levels using the curve fitting method. This may be possible because the peak pk#3 is broader and thus has a higher probability of containing multiple traps. The trap level at 0.20 eV is tentatively identified as EL14, EL9 [10]. The corresponding capture-cross section ($1.7\times10^{-15}$ $cm^2$) also agrees with the results obtained by other researchers [10]. The trap level at 0.32 eV is tentatively identified as EL6 [10]. The levels at 0.48 eV and 0.30 eV are obtained around 330K using the

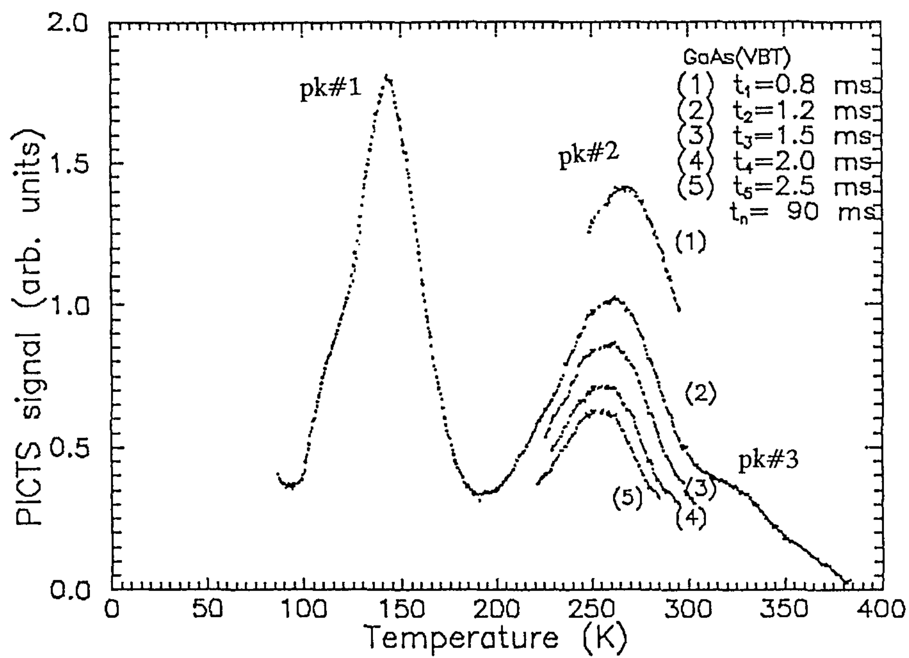


(a)

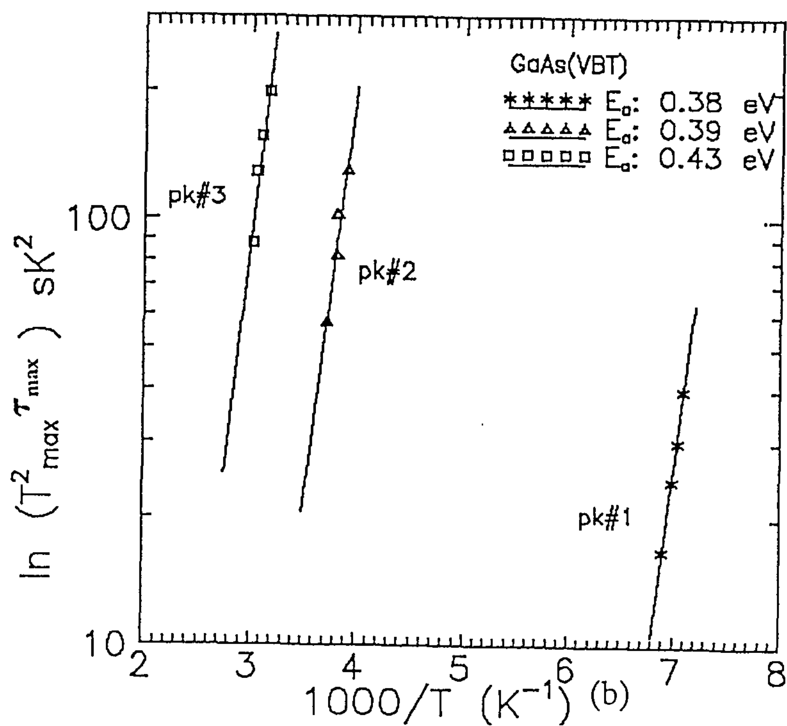


(b)

Fig. 14 (a) A typical PICTS spectrum of GaAs(VBT grown) sample (b) An arrhenius plot of GaAs(VBT grown) obtained using the rate window method.

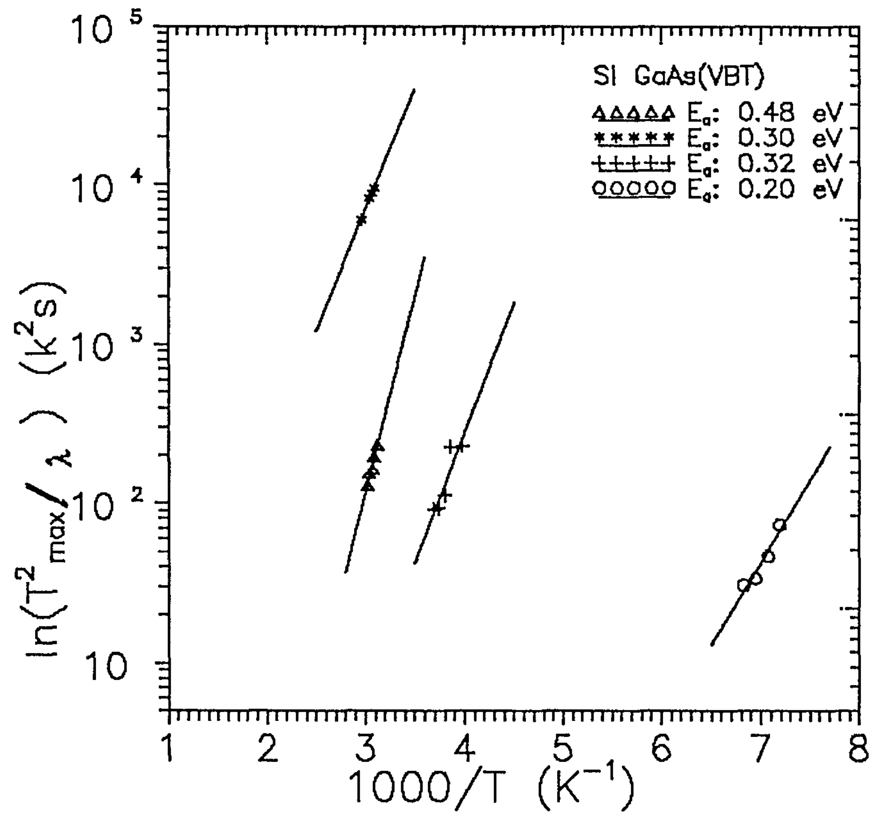


Fig. 14 (c) An arrhenius plot of GaAs(VBT grown) obtained using the curve fitting method.

curve fitting method. The level at 0.38 eV obtained using the rate window technique corresponds to EL5 [33]. This defect level is also observed by Martin *et al.* in their work [34].

**GaAs:Cr sample**

The PICTS spectrum of chromium doped GaAs (Fig. 15(a)) shows three well-defined peaks with activation energies of 0.61 eV, 0.51 eV, and 0.16 eV. These are identified as EL12, EL3, and EL10, respectively, and are in agreement with the published results [11-14]. The level at 0.61 eV is resolved into 0.63 eV and 0.59 eV employing the curve fitting method. The level at 0.63 eV is due to chromium impurity and tentatively identified as an acceptor level [35]. The level at $0.59 \pm 0.03$ eV was reported by Martin *et al.* for their EL3 electron trap for GaAs:Cr. This is also noted by Fairman *et al.* for the bulk GaAs:Cr sample. The peak pk#1 is resolved into two trap levels, 0.21 eV and 0.14 eV by using the curve fitting method. The level at 0.21 eV ($0.23 \pm 0.03$ eV) is observed by other researchers; however, the signature of the trap is not identified [11].

***DISCUSSIONS***

The results obtained from the deep level characterization using both the rate window and the curve fitting technique are tabulated in Table 3 and Table 4

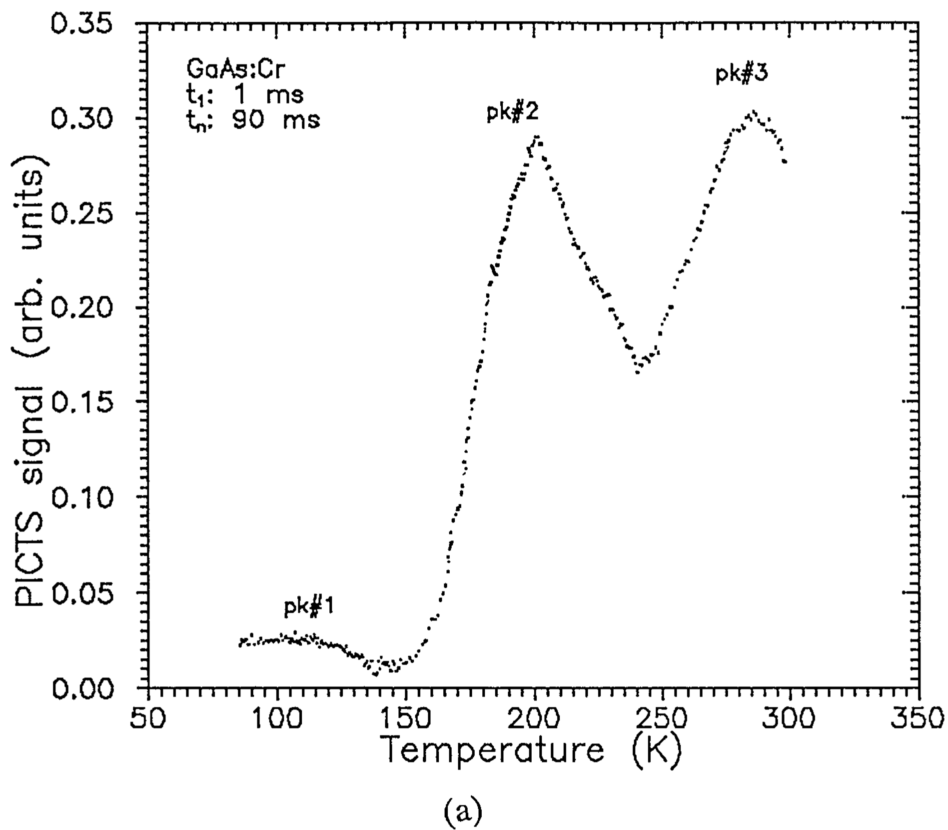


(a)

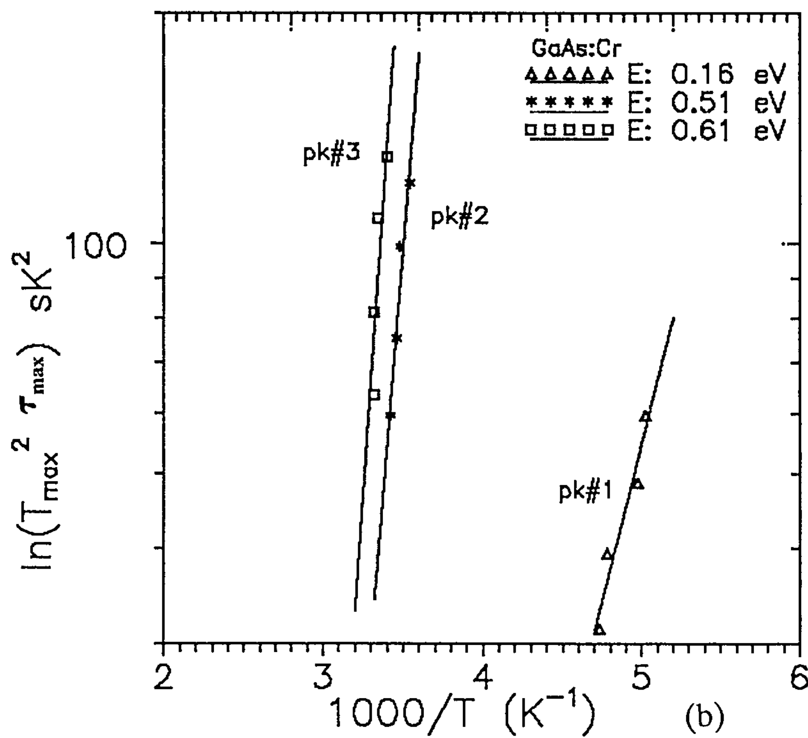


(b)

Fig. 15 (a) A typical PICTS spectrum of Cr-doped GaAs sample
(b) An arrhenius plot of GaAs:Cr sample using the rate window method.

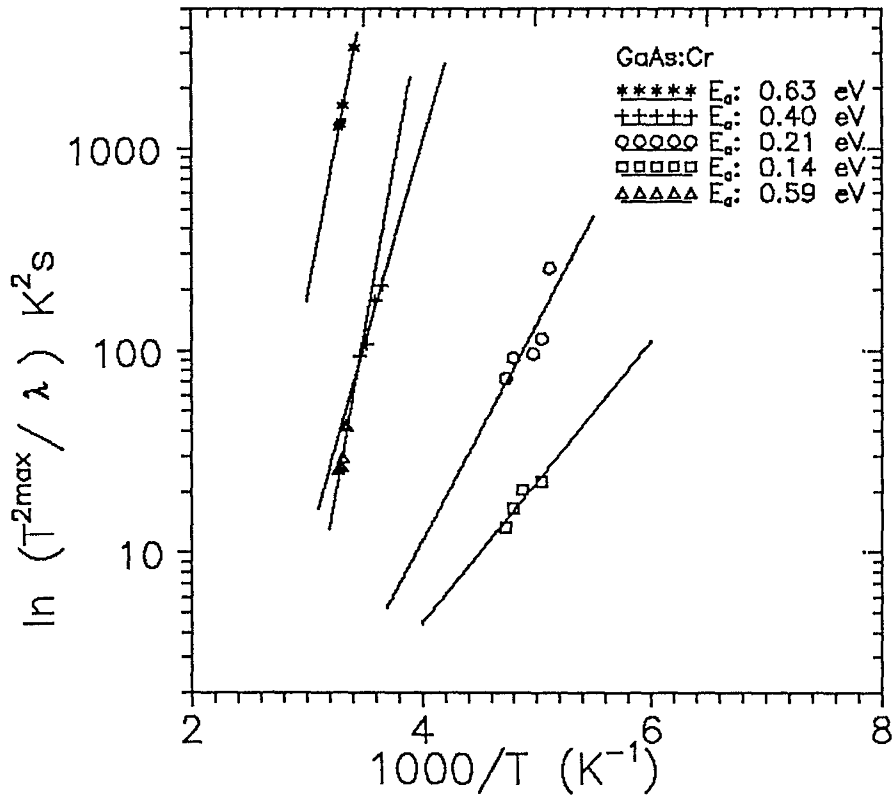


Fig. 15 (c) An arrhenius plot of GaAs:Cr obtained using the curve fitting method.

respectively. The signature of the trap levels is also shown in the table except a few which are not yet identified. The activation energy ($E_a$) of both the methods is shown in Table 5 for comparison purposes. As seen from the results, there is a large variation in trap energy level obtained from the two techniques. The main reason for this discrepancy can be attributed to the assumption of a single exponential decay considered in two-gated rate window method for the determination of trap parameters. In other cases even though a peak is not resolved into number of exponentials, different values for trap parameters, (e.g. LEC-grown GaAs, 0.21 eV for rate-window and 0.28 eV for curve fitting) are obtained. This observation is not unique. Similar observations are also made by other researchers in their work [10,15]. However, in many cases the peaks are resolved into a number of closely spaced levels, a result which is otherwise not possible by using the two-gated rate window method. Thus, it is seen that fitting of the transient provides more information than use of the rate window method. The value of capture cross-section ($\sigma_n$ or $\sigma_p$) obtained using the two-gated rate window method is abnormally higher than that obtained using the curve fitting method. Similar observations are also made by Brasil *et al.* in their work [10]. This difference may be due to the assumption of single exponential decay made in the rate window method. An important observation is that although EL2 is a major trap level in GaAs, it is not detected in the GaAs:Si:Cu, GaAs (VBT grown), and GaAs:Cr sample studied in the present work.

Table 4. Deep level parameters obtained using the curve fitting method.

| Sample | Activation Energy (eV) | Capture Cross- section ($\sigma$)cm$^2$ |
|---|---|---|
| SI GaAs | 0.80 | $7.5 \times 10^{-15}$ |
| | 0.27 | $3.7 \times 10^{-18}$ |
| | 0.42 | $2.12 \times 10^{-17}$ |
| GaAs (LEC) | 0.66 | $6.96 \times 10^{-14}$ |
| | 0.61 | $9.00 \times 10^{-13}$ |
| | ------------ | ------------ |
| | 0.57 | $11.30 \times 10^{-11}$ |
| | 0.55 | $2.75 \times 10^{-11}$ |
| | ------------ | ------------ |
| | 0.28 | $4.32 \times 10^{-14}$ |
| GaAs (VBT) | 0.48 | $9.30 \times 10^{-16}$ |
| | 0.30 | $2.27 \times 10^{-20}$ |
| | ------------ | ------------ |
| | 0.32 | $5.57 \times 10^{-17}$ |
| | ------------ | ------------ |
| | 0.20 | $1.70 \times 10^{-15}$ |
| GaAs:Cr | 0.63 | $5.58 \times 10^{-12}$ |
| | 0.59 | $2.20 \times 10^{-14}$ |
| | ------------ | ------------ |
| | 0.40 | $4.40 \times 10^{-16}$ |
| | ------------ | ------------ |
| | 0.21 | $7.98 \times 10^{-18}$ |
| | 0.14 | $6.10 \times 10^{-18}$ |

Table 5. A Comparison of deep level parameters between the rate window method and the curve fitting method of SI GaAs sample.

| Sample | Trap Level | Rate Window Method<br>Activation Energy ($E_a$) eV | Curve Fitting Method<br>Activation Energy ($E_a$) eV |
|---|---|---|---|
| SI GaAS | EL2 | 0.78 | 0.80<br>0.27<br>0.42 |
| GaAs (LEC) | EL2 | 0.85 | 0.66<br>0.61 |
| | ? | 0.63 | 0.57<br>0.55 |
| | ? | 0.21 | 0.28 |
| GaAs (VBT) | ? | 0.43 | 0.48<br>0.30 |
| | ? | 0.39 | 0.32 |
| | ? | 0.38 | 0.20 |
| GaAs (CR) | ? | 0.61 | 0.63<br>0.59 |
| | ? | 0.51 | 0.40 |
| | ? | 0.16 | 0.21<br>0.14 |

It is observed that multiple traps are present in a particular temperature range. This may be possible because the trap center resonance not only depends on temperature but also on the capture cross-section of the trap. The multiple decay time constants obtained from the computation indicate that the transients consist of the sum of exponentials throughout the temperature range centered around the resonance peak. This method can separate out closely spaced traps which is not possible in two-gated rate window method. Since the decay constants are obtained directly from the transients, trap parameters calculated employing the curve fitting method are more accurate and reliable than those obtained from the two-gated rate window method. However, if the transients are approximately exponential in nature, the rate window technique provides a trap energy level. This observation can be verified from the results obtained from the curve fitting method [Table 4]. In this aspect, the rate window method has an edge over the curve fitting method because the computation time can be minimized.

## *SOURCES OF ERROR AND ANALYSIS*

Analysis of current transients can provide a quick and relatively easy way to obtain deep level parameters present in the sample. However, several problems exist both in the analysis of the data and its limited usefulness and applicability. During analysis it is required to select the region of the transient to be fitted exponentially. Although, the program selects the initial and final value of the current transient, it

is essential to adjust both the points interactively during program execution until a best fit is observed. This process is an eye estimation only and hence can introduce error in judgement.

Finite resolution affects any measurement using discrete numbers. All digital storage devices store amplitude values as discrete numbers and associate those amplitude numbers with discretely numbered times. Many measurements must be rounded or truncated. The size of the truncation or rounding becomes a part of measurement error. There are several places where measurements are quantified, and a one-count error in the measurement cannot be detected. The input channels are digitized to an 8-bit resolution in tektronix-2232 oscilloscope, where one division is 25 counts in the sample mode. This means there is an inherent error of 1/25 of a division in any voltage waveform at acquisition time. The signal can be averaged in the oscilloscope, and this averaged signal has a resolution of 100 points per division with an error of 1/100 of a division. The error in this digital storage with 8-bit resolution is more than the 12 bit resolution of AD500 (A/D conversion electronics) used earlier in the rate-window technique. Therefore, a good digitizer with 16-bit or higher resolution may improve the accuracy of measurement.

The capture cross-section ($\sigma_n$) is calculated using the equation 2.9. The factor $\gamma_n$ in the equation is assumed to be independent of temperature and used approximately as a constant. In addition, the capture cross-section depends on an electric field, the effect of which has not been considered in the calculations for

simplicity. These approximations have introduced further inaccuracies in the capture cross-section calculation.

The recombination lifetime ($\tau_n$) of carriers or electrons has been considered to be independent of other influencing factors, such as recombination lifetime of carriers, which in turn depends on the availability of free carriers of opposite polarity; the temperature of the semiconductor sample; inversely on the concentration of the recombination center; and capture cross-section. Calculation of trap concentration is really complex if all the factors are taken into consideration for evaluation. Therefore, for simplicity of calculation, a recombination lifetime of 10 *ns* has been used in the computation. Approximately two orders of magnitude error in carrier concentration can be introduced by using a constant value of carrier recombination lifetime (10 *ns*).

Sufficient care must be taken to avoid injection of minority carriers into the sample, which can result in measurement errors. This problem can arise if the laser beam is not exactly focused on the non-contact part of the sample. The problem is quite inevitable in our system because the styrofoam insulation around the cryogenic cell contracts and expands with the change of temperature. As a result, there is a possibility of a laser beam being out of focus during the experiment and shining on the contact. The problem is more severe in the case of samples with a small gap between the contacts.

In our trap concentration calculation, a constant $\mu\tau$ product has been assumed, an assumption which introduces error in the calculation for the following

reasons. The mobility changes with temperature. The conductivity mobility determines the conductivity or the resistivity of a semiconductor material. While computing the carrier concentration of a trap level, a constant mobility of 8000 $cm^2/V$-s (for GaAS) and 900 $cm^2/V$-s (for ZnSe) has been used in the equations for simplicity, which are actually hall mobilities. Hall mobility, which is determined from hall-effect, differs by a factor (approximately 2 times) and is dependent on the scattering mechanism. This scattering mechanism, very common in GaAs, often limits the mobility of carriers and depends on geometry, contact size, and inhomogeneity of the sample. In view of these reasons, the actual conductivity mobility of SI GaAs is less than 8000 $cm^2/V$-s, and this approximation can introduce an order of magnitude error in the carrier concentration computation.

## *CONCLUSIONS*

A detailed analysis of photo induced current transient spectroscopy on high-resistivity material using a novel technique is discussed. The results obtained using both the rate window and the curve fitting method are discussed and compared. It is observed that the curve fitting method can separate out closely spaced traps within the bandgap, otherwise not possible in the conventional two-gated rate window method.

An important result obtained in this work is the detection of the $Cu_A$ level in the GaAs:Si:Cu material, for the first time, in our laboratory. This information

obtained provides the feedback necessary for modifications in the processing condition so that the partition ratio ($N_{CuB}$ / $N_{CuA}$) can be fine tuned to obtain best switching performance. Since the properties of the $Cu_B$ level play an important role in the performance of BOSS switch, compensation achieved predominately by other levels may degrade the switch performance. In this context, detection of $Cu_A$ level is vital because the $Cu_A$ and $Cu_B$ concentrations are inter-related. Polycrystalline ZnSe as a switch material has not been fully investigated. However, the deep level parameters obtained are a guideline for modelling of ZnSe as a switch material for pulsed power applications.

The digital approach to data acquisition solved some of the earlier experimental problems. The number of data points per transient has been increased from 512 to 1024, signal to noise ratio (S/N) is improved, and the system can generate multiple PICTS spectra in a single thermal cycle. However, a high resolution digitizer (16-bit or higher) may improve the data quality for better result.

Our analysis indicates that multiple trap levels can be determined by the curve fitting method, which is an alternative and more reliable method. However, we cannot disregard the two-gated rate window method completely. The PICTS spectrum qualitatively provides an idea about traps present in the sample which can be used as a guideline for the curve fitting analysis. At present, the curve fitting of transients obtained from PICTS measurement seems to be the most attractive technique for determination of deep level parameters.

*SCOPE OF FUTURE WORK*

In the following section, a brief discussion on suggestions for future work toward achieving better performance of the system from the point of view of reliability of the BOSS CRYOGENIC CELL is presented. Generally, during PICTS measurements, the cold finger temperature varies approximately from 77K (boiling point of liquid nitrogen) to 425K or higher. The signal cable rests on the cold finger of the cryogenic cell, which acts as a mechanical support and is soldered to the sample. Therefore, the signal cable is subjected to very wide range of thermal stress during the experiment and can result in insulation failure, causing a short circuit with the ground. This problem is inevitable after three or four thermal cycles and requires frequent replacement of the signal cable. The major drawback is that the whole experiment is stopped if a short circuit occurs during the experiment. Therefore, suitable modification is necessary on the cold finger to support the signal cable. In addition, the cryogenic cell is covered with styrofoam which acts as thermal insulation to the cell. The styrofoam contracts and expands with the change of temperature during the experiment and disturbs the laser alignment with respect to the sample. This interrupts the experiments since a realignment results in restarting of the experiment.

There are difficulties in the curve fitting method which affect the method of analysis. Sometimes, minima and maxima which are observed in the current transients, may be due to the presence of random noise in the signal. The technique

can not be applied to those transients which have such noise. In addition, the chi-square minimization procedure (ref. Appendix-A) is based on the assumption of normally distributed (gaussian) noise in the signal (current transient), which is not always the case. This problem can be reduced to a great extent by a detailed analytic calculation in determining which contour $\Delta\chi^2$ is the correct one for the desired confidence level.

## REFERENCES


[1] S.M. Sze, "*Semiconductor devices, physics and technology*," John Wiley and Sons, New York, 1985.

[2] P.T. Ho, Feng Peng, and J. Goldhar, "Photoconductive Switching using Polycrystalline ZnSe," *IEEE Transaction on Electron Devices*, vol. 37, pp. 2517-2519, 1990.

[3] R.P. Brinkmann and K.H.Schoenbach, "Electron-Beam controlled Switching with wide bandgap Semiconductors," *8th IEEE International Pulsed Power Conference*,San Diego, California, pp. 94-101, 1991.

[4] S.M. Sze, "*VLSI Technology*," McGraw Hill Book Company, New York, Second edition, 1988.

[5] D. K. Schroder, "*Semiconductor Material Characterization,*" Wiley & Sons, New York, 1990.

[6] P. Hlinomaz, V. Smid, J. Kristofik, J.J. Mares, P. Hubik, J. Zeman, "A Comparison of PICTS with direct measurement of non-exponential current transients on SI GaAs," *Solid State Communications*, Vol. 77, pp. 409-413, 1991.

[7] G.R. Barevadia, "*Deep Level Characterization Studies In GaAs*," M.S. Thesis Dept. of Electrical and Computer Engineering, Old Domonion University, Norfolk, Virginia, 1990.

[8] Brinkmann R.P. , Private communication.

[9] Richard H. Bube, "*Photoconductivity of Solids*," John Wiley & Sons, 1960.

[10] Maria J.S.P. Brasil and P. Motisuke, "Deep center characterization by photo-induced transient spectroscopy," *J. Appl. Phys.* vol. 68, pp. 3370-3376, 1990.

[11] J.C. Abele, R.E. Kremer, and J.S. Blakemore, "Transient Photoconductivity Measurements in Semi-insulating GaAs. I. An Analog Approach II. A Digital Approach," *J. Appl. Phys*. vol. 62, pp. 2432-2438, 1987.

[12] K. H. Schoenbach, V. K. Lakdawala, R. Germer, and S. T. Ko, "An optically controlled closing and opening semiconductor switch," *J. Appl. Phys.*, vol. 63, pp. 2460-2463, 1988.

[13] V. K. Lakdawala, L. M. Thomas, S. Panigrahi, K.H. Schoenbach, G. R. Barevadia, W. M. Money, "Deep level parameter studies and their significance for optically controlled solid state switches," *Proc. 8th IEEE Pulsed Power Conf.*, San Diego, CA, pp. 1032-1036, 1991.

[14] M. R. Burd and R. Braunstein, "Deep Levels in semi-insulating Liquid Encapsulated Czochralski-grown GaAs," *J. Phys. Chem. Solids*. vol. 49, pp. 731-735, 1988.

[15] D.C. Look, *"Electrical Characterization of GaAs Materials and Devices,"* Wiley & Sons, New York, 1989.

[16] J. C. Balland, J. P. Zielinger, M. Tapiero, J. G. Gross, and C. Noguet, "Investigation of deep levels in high-resistivity bulk materials by photo-induced current transient spectroscopy: II. Evaluation of various signal processing methods," *J. Phys, D: Appl. Phys.*, vol. 19, pp. 71-87, 1986.

[17] Maria J.S.P. Brasil and Paulo Motisuke, "Direct Analysis of the Photocurrent Transient in Semi-Insulating GaAs," *Solid state communications*, vol. 74, pp. 935-939, 1990.

[18] Chris Spatz, James O. Johnston, "*Basic statistics*," Second edition Brooks/ Cole publishing company, Monterey, California, 1981.

[19] Clark A. Hawkins, Jeans E. Weber, "*Statistical Analysis*," Harper and Row publishers, New York, 1980 .

[20] Ralph B. D'Agostino, Michael A. Stephens, "*Goodness-of-fit Techniques*," Marcel Dekker, New York, 1986.

[21] William H. Press, Saul A. Teukolsky, Brian P. Flannery, and William T. Vettering, "*Numerical Recipes, The art of scientific computing*," Press syndicate of the University of Cambridge, New York, 1986.

[22] P.K.Lim and D.E.Brodie, "An electronic structure for a ZnSe," *Canadian Journal of Physics*, Vol. 55, pp 1641 - 1647, 1977.

[23] S. T. Ko, V. K. Lakdawala, K. H. Schoenbach, and M. S. Mazzola, "Influence of copper doping on the performance of optically controlled GaAs switches," *J. Appl. Phys.*, vol. 67, pp. 1124-1126, 1990.

[24] S.M. Sze, "*Physics of Semiconductor Devices*," John Wiley & Sons, New York, 1981.

[25] N.Kullendoorff and L. Jansson, "Copper-related deep level defects in III-V semiconductors," *J. Appl. Phys.* vol. 54(6), pp. 3203 - 3212, 1988.

[26] C.C. Tin, C.K. Teh, and F.L.Weichman, "States of Copper during diffusion in semi-insulating GaAs," *J. Appl. Phys.* vol. 63(2), pp.355-359, 1988.

[27] H.J. Queisser and C.S. Fuller, "Photoluminescence of Cu-doped Gallium arsenide,"*J. Appl. Phys.* vol. 37, pp. 4895-4899, 1966.

[28] Joseph Blanc, Richard H. Bube, and Harold E. MacDonald, "Properties of High-Resistivity Gallium Arsenide Compensated with diffused copper," *J. Appl. Phys.*, vol. 32(9), pp. 1666-1679, 1961.

[29] V.K. Lakdawala, Sridhar Panigrahi, Lucy M. Thomas, and Ralf Peter Brinkmann, "Deep level characterization studies for optically controlled semiconductor switch materials using a novel technique," Proc. SPIE conference on optically activated switching, Los Angeles, California, Jan' 92.

[30] Paul Besomi and Bruce W. Wessely, "Deep level defects in heteroepitaxial Zinc Selenide," *J. Appl. Phys.* vol. 53, pp. 3076-3084, 1988.

[31] Kiyoshi Yoneda, Yuji Hishida, and Hiroaki Ishii, "Deep electron traps in undoped, molecular beam epitaxially grown ZnSe," *Appl. Phys. Lett.*, vol. 47(7), pp. 702-704, 1985.

[32] S.R. Blight, H. Thomas, "Investigation of the Negative peak in photoinduced transient spectra of semi-insulating gallium arsenide," *J. Appl. Phys.* vol. 65, pp. 215-226, 1989.

[33] P. Hlinomaz, V. Smid, J. Kristofik and J.J. Mares, "Comparison of different types of signal processing in PICTS measurement," *Journal of solid state communication*, vol. 78, pp. 947-951, 1991.

[34] G.M. Martin, A.Mitonneau, and A.Mircea, "Electron traps in bulk and epitaxial GaAs crystal," *Electron Lett.* vol. 13, pp. 191-193, 1977.

[35] Sherif Makram-Ebeid, Brian Tuck, "*Semi-insulating III-V Materials,*" Evian Shiva Publishing Limited, England, 1982.

[36] M. Tapiero, N. Benjelloun, J.P. Zielinger, S. El Hamd, and C. Noguet, "Photoinduced Current Transient Spectroscopy in High-resistivity bulk

Materials: Instrumentation and methodology," *J. Appl. Phys*. vol. 64, pp. 4006-4012, 1988.

[37] J. C. Balland, J. P. Zielinger, C. Noguet and M. Tapiero, "Investigation of deep levels by photo-induced current transient spectroscopy: I. Review and analysis of some basic problems," *J. Phys. D: Appl. Phys.* vol. 19, pp. 57-70, 1986.

[38] M. S. Mazzola, K. H. Schoenbach, V. K. Lakdawala, and S. T. Ko, "Nanosecond optical quenching of photoconductivity in a bulk GaAs switch," *Appl. Phys. Lett.*, vol. 55, pp. 2102-104, 1989.

[39] O. Yoshie & M. Kamihara, "Photo-Induced Current Transient Spectroscopy in high resistivity bulk material," *J. Appl. Phys*. vol. 24, pp. 431-440, April, 1985.

[40] V. K. Lakdawala, K. H. Schoenbach, R. A. Roush, G. R. Barevadia, and M. S. Mazzola, "Photoquenching and characterization studies in a bulk optically controlled GaAs semiconductor switch," *Proc. SPIE Proceedings of the OPTCON'90*, Boston , vol. 1378, pp. 259-270, 1990.

[41] L. M. Thomas, V. K. Lakdawala, and S. Panigrahi, "Influence of arsenic vapor pressure during copper diffusion on deep level formation in silicon doped gallium arsenide," *submitted to J. Mater. Sci.* 1992.

[42] GaAs samples purchased from Lawrence Livermore Laboratory, CA.
Specifications:
(i) GaAs (Vertical Bridgman Technique)
Semi-insulating V48-37, Bulk Material, 1 mm thick, Grown in Lab.
Undoped, Orientation: <100>
(ii) LEC GaAs (HP-12-17-90, Druce), 2 mm.
SI Bulk Material, Grown by Showa Denko (Japan), Undoped
Orientation: <100>
Hall Mobility: $7 x 10^3$ $cm^2/V$-S
(iii) GaAS: Cr - (HP-6-7-90, #Y0485-T3), 3 mm thick,
SI-Bulk Material, Orientation: <100>, Etch density $<10^5/cm$
Grown by FURUKAWA of Japan.

[43] Z-Q. Fang and D.C. Look, "Comparison of deep centers in SI LEC and vertical gradient freez GaAs," *J. Appl. Phys*. vol. 69(12), pp. 8177-8182, 1991.

[44] U.V. Desnica, Dunjan I. Desnica, and B. Santic, "EL2 related deep traps in semi-insulating GaAs", *Appl. Phys. Lett*. vol. 58(3), pp. 278-280, 1991.

[45] F.D. Auret, A.W.R. Leitch, and J.S. Vermaak, "A DLTS analysis of electron-hole traps in bulk GaAs," *J. Appl. Phys.* vol. 59(1), pp. 158-163, 1986.

## APPENDIX-A

Modeling of polynomials or gaussians by adjustable parameters is discussed in this appendix. The basic approach in all cases is usually to design a figure-of-merit function that measures the agreement between the data and the model with a particular choice of parameters. The parameters of the model are then adjusted to achieve a minimum in the merit function yielding best fit parameters. The adjustment process is thus a problem in minimization in many dimensions. Besides this data are generally not exact and subjected to measurement errors such as noise. Even though the model is correct, the data may not exactly fit the model. In this situation we asses whether or not a model is appropriate by taking help of some useful statistical standard i.e. test the goodness-of-fit. Here we need to know the likely errors of the best-fit parameters. Therefore, a fitting procedure should provide the following features such as (i) parameters (ii) error estimates on the parameters (iii) a statistical measure of goodness-of-fit [21].

**Least Square as a Maximum Likelihood Estimator:**

Suppose we are fitting N data points such as $(x_i,y_i)$, $i = 1.......N$, to a model which has M adjustable parameters $a_j$, $j = 1.........M$. The model predicts a functional

relationship between the measured independent and dependent variables as given in the following equation.

$$y(x) = y(x;\ a_1 \ldots\ldots\ldots\ldots\ldots\ldots\ldots a_M) \qquad \text{(A.1)}$$

To obtain fitted values for the $a_j$'s we need to minimize over $a_1 \ldots\ldots\ldots a_M$ :

$$\sum_{i=1}^{N} \left[ y_i - y\ (\ x_i\ ;\ a_1 \ldots\ldots\ldots a_M\ )\right] 2 \qquad \text{(A.2)}$$

This process is known as least square fit and this is based on the principle called maximum likelihood estimators. Given a particular data set of $x_i$'s and $y_i$'s, we have the intuitive feeling that some parameter sets $a_1 \ldots\ldots\ldots a_M$ are very unlikely those for which the model function y(x) looks nothing like the data, while the others may be very likely, those which closely resemble the data. Now question comes; what is the probability that a particular set of fitted parameters $a_1 \ldots\ldots\ldots a_M$ is correct? There is just one model, the correct one, and a statistical universe of data sets that are drawn from it. Conversely, our intuition tells us that the data set should not be too improbable for the correct choice of parameters. In other words, we identify the probability of the data given the parameters, as the likelihood of the parameters given the data. There is no formal mathematical basis in it.

Suppose that each data point $y_i$ has a measurement error that is independently random and distributed as a normal (gaussian) distribution around the "true" model y(x). Suppose the standard deviation sigma ($\sigma$) of these normal distributions are the same for all points. Then the probability of the data set is the product of the probabilities of each point given by the following relation.

$$P = \prod_{i=1}^{N} \exp\left[-\frac{1}{2}\left(\frac{y_i - y(x_i)}{\sigma}\right)^2\right] \Delta y \tag{A.3}$$

We need to maximize the equation A.3. By taking log of both sides and simplifying we have the following relation.

$$-\log_e P = \left[\sum_{i=1}^{N} \frac{[y_i - y(x_i)]^2}{2\sigma^2}\right] - N \log \Delta y \tag{A.4}$$

Maximization of equation A.3 is same as minimizing the right hand side of equation A.4 i.e. negative of its logarithm. Since N, $\sigma$, and y are all constants, minimizing this equation A.4 means minimizing equation A.2.

We noticed that least-square fitting is a maximum likelihood estimation of the fitted parameters if the measurement errors are independent and normally distributed with constant standard deviation. In the above the linearity or nonlinearity of the model is not considered. Now we will relax our assumption of constant standard deviations and obtain new procedure called "Chi-Square fitting" or "weighted least-square fitting."

# APPENDIX-B

## Chi-Square Fitting

Suppose we have N data points ($x_i$, $y_i$) and each point has its own standard deviation $\sigma_i$ . Then the equation (called "Chi-square") is modified as follows.

$$\chi^2 = \sum_{i=1}^{N} \left( \frac{y_i - y\,(x_i\ ,\ a_1 \ldots\ldots a_M)}{\sigma_i} \right)^2 \qquad \textbf{(B.1)}$$

To the extent measurement errors actually are normally distributed, the quantity $\chi^2$ is the sum of N squares of normally distributed quantities, each normalized to unit variance. Once we have adjusted the $a_1 \ldots\ldots a_M$ to minimize the values of $\chi^2$, the terms in the sum are not all statistically independent. The probability distribution for different values of $\chi^2$ at its minimum is the Chi-Square distribution for N-M degrees of freedom, where N is the number of data points and M is the number of adjustable parameters.

Let $\nu$ = N-M , an integer known as the degrees of freedom.

$P(\chi^2/\nu)$, the probability that the observed Chi-Square for a correct model should be less than a value $\chi^2$.

$Q(\chi^2/\nu)$ - Defined as the complement of P, and is the probability that the observed Chi-Square will exceed the value $\chi^2$ by chance even for a correct model.

The functions have the limiting values as follows.

$P(0/\nu) = 0 \qquad P(\infty/\nu) = 1$

$Q(0/\nu) = 1 \qquad Q(\infty/\nu) = 0$

Therefore, $\quad P = 1 - Q$

If Q is a very small probability of some particular data set, then the apparent discrepancies are unlikely to be chance fluctuations. There is probability that either (i) model is wrong i.e. model is statistically rejected (ii) the size of measurement error $\sigma_i$ is much larger than considered (iii) is fairly common. Sometimes it may be such that Q is nearly equal to 1 , i.e. too good to be true. In this case measurement error is too high, which normally doesn't happen. Therefore, the cause of too good a chi-square fit is that the measurement error has been overestimated.

As per thumb rule, a "typical" value of $\chi^2$ for a "moderately" good fit is $\chi^2$ = $\nu$ (degree of freedom). Now if we take the derivative of the equation B.1 with respect to the parameters $a_k$, we obtain equations (B.2) which must hold at the Chi-square minimum.

$$0 - \sum_{i-1}^{N}\left(\frac{y_i - y(x_i)}{\sigma_i^2}\right)\left(\frac{\partial y(x_i \;,\ldots\ldots\ldots a_k \ldots)}{\partial a_k}\right) \; (k-1\ldots\ldots M\;) \qquad \textbf{(B.2)}$$

The equation B.2 has a set of M nonlinear equations for the M unknowns $a_k$.

# APPENDIX-C

## NONLINEAR MODELS

Now consider fitting when the model depends nonlinearly on the set of M unknown parameters $a_k$, k=1,2,.....M. We use the same approach to define a $\chi^2$ merit function and determine best-fit parameters by its minimization. With nonlinear dependence, however, the minimization must proceed iteratively. The procedure is then repeated until $\chi^2$ stops or effectively stops decreasing. When the $\chi^2$ function is close to minimum it can be well approximated by a quadratic form, which can be written as,

$$\chi^2(\mathbf{a}) \approx \gamma - \mathbf{d}.\mathbf{a} + (1/2)\ \mathbf{a}.\mathbf{D}.\mathbf{a} \qquad \text{(C.1)}$$

where **d** is an M-vector and **D** is an M x M matrix. If the approximation is a good one, then it is possible to jump from current trial parameters $a_{cur}$ to the minimizing ones $a_{min}$ in a single step which is given by the following relation.

$$\mathbf{a}_{min} = \mathbf{a}_{cur} + \mathbf{D}^{-1}.[-\nabla\chi^2(\mathbf{a}_{cur})] \qquad \text{(C.2)}$$

We must be able to compute the gradient of the $\chi^2$ at any set of parameters **a** . To use equation 11 we also need the matrix **D**, which is the second derivative matrix (Hessian matrix) of the $\chi^2$ merit function, at any a.

The model to be fitted is;

$$y = y(x;a) \tag{C.3}$$

and the chi-square merit function is,

$$\chi^2(a) = \sum_{i=1}^{N} \left[\frac{y_i - y\ (x_i\ ;\ a)}{\sigma_i}\right]^2 \tag{C.4}$$

The gradient of $\chi^2$ with respect to the parameters **a**, which will be zero at the $\chi^2$ minimum, has components,

$$\frac{\partial \chi^2}{\partial a_k} = -2\sum_{i=1}^{N} \frac{[y_i - y(x_i\ ;\ a)]}{\sigma_i^2} \frac{\partial y(x_i\ ;\ a)}{\partial a_k} \tag{C.5}$$

Taking an additional partial derivative gives,

$$\frac{\partial^2 \chi^2}{\partial a_k \partial a_l} = 2\sum_{i=1}^{N} \frac{1}{\sigma_i^2}\left[\frac{\partial y(x_i\ ;\ a)}{\partial a_k}\frac{\partial y(x_i\ ;\ a)}{\partial a_l} - [y_i - y(x_i\ ;\ a)]\frac{\partial^2 y_i(x_i\ ;\ a)}{\partial a_l \partial a_k}\right] \tag{C.6}$$

It is conventional to remove the factors of 2 by defining,

$$\beta_k = -\frac{1}{2}\frac{\partial \chi^2}{\partial a_k}, \qquad \alpha_{kl} = \frac{1}{2}\frac{\partial^2 \chi^2}{\partial a_k\ \partial a_l} \tag{C.7}$$

making $[\alpha] = (1/2)\mathbf{D}$ in equation (C.2), in terms of which that equation can be written as the set of linear equations

$$\sum_{i=1}^{M} \alpha_{kl}\ \delta_{al} = \beta_k \tag{C.8}$$

This set is solved for the increments $\delta a_l$ that, added to the current approximation, give the next approximation. In the context of least-squares, the matrix $[\alpha]$, equal to one-half times the Hessian matrix, is usually called the curvature matrix.

The steepest descent equation can be written as $\delta a_l$ = constant $\times \beta_l$. The condition at the $\chi^2$ minimum, that $\beta_k = 0$ for all k, is independent of how $[\alpha]$ is defined.

Levenberg-Marquardt Method

Levenberg-marquardt method works very well for non-linear least-squares routines. The recommended recipe for an initial guess for the set of fitted parameters **a** is as follows:

(i) compute $\chi^2$ (a)

(ii) pick a modest value for $\lambda$, say $\lambda = 0.001$

(iii) solve linear equations $\Sigma_{l=1}^{M} a_{kl'}\ \delta a_l = \beta_k$ for $\delta a$ and evaluate $\chi^2(a+\delta a)$.

(iv) If $\chi^2(a+\delta a) \geq \chi^2(a)$, increase $\lambda$ by a factor of 10 and go back to step (iii)

(v) If $\chi^2(a+\delta a) < \chi^2(a)$, decrease $\lambda$ by a factor of 10, update the trial solution a---a+$\delta$a, and go back to (iii).

Also necessary is a condition for stopping. Iteration to convergence is generally wasteful and unnecessary since, the minimum is at best only a statistical estimate of the parameters a. The change in the parameters that changes $\chi^2$ by an amount $<< 1$ is never statistically meaningful.

It is sometimes not uncommon to find parameters wandering around near the minimum in a flat valley of complicated topology. More often, a small pivot will generate a large correction which is then rejected, the value of $\lambda$ being then

increased. For sufficiently large $\lambda$ the matrix $[\alpha']$ is positive definite and can have no small pivots. Thus, the method does tend to stay away from zero pivots, but at the cost of a tendency to wander around doing steepest descent in very un-step degenerate valleys. These considerations suggest that, in practice, one might as well stop iterating on the first or second occasion that $\chi^2$ decreases by a negligible amount, say either less than 0.1 absolutely or some fractional amount like $10^{-3}$. One should not stop after a step where $\chi^2$ increases: that only shows that $\lambda$ has not yet adjusted itself optimally.

Once the acceptable minimum has been found, one wants to set $\lambda=0$ and compute the matrix $[C] \equiv [\alpha]^{-1}$ , which is the estimated covariance matrix of the standard errors in the fitted parameters **a**.

A pair of subroutine MRQMIN and MRQCOF in the program (appendix-C) encodes Marquardt's method for non-linear parameter estimation. It is first called (once) with ALAMDA < 0, which signals the routine to initialize. ALAMDA is returned on the first and all subsequent calls as the suggested value of $\lambda$ for the next iteration. When convergence is deemed satisfactory, the program set ALAMDA to zero before a final call. The routine MRQMIN calls the routine MRQCOF for the computation of the matrix $[\alpha]$ and vector ß. In turn MRQCOF calls the user-supplied routine FUNCS which for the vector of derivatives DYDA $\equiv \Delta y/\Delta a_k$.

A flow chart of the program is shown in page 91 for computation of amplitude ($C_k$) and decay time constant ($\lambda_k$) for non-linear models. In fact, the number of data points to be fitted are adjusted interactively by selecting the initial ($f_q$) and final ($f_p$)

point in the transients. The program computes the $C_k$ and $\lambda_k$ and plots the modes, known as statistically confirmed parameter set. Each mode is plotted with a number of ellipsoids and the boundary of the ellipses represent the confidence limits.

Chi-square boundaries as confidence limits

This section describes the meaning of quantitative uncertainties and give further information to estimate the confidence limit on the fitted parameters. Here the data is fitted by $\chi^2$ minimization and the fitted parameters are denoted as $a_{(0)}$. When the method is used to estimate the parameters $a_{(0)}$, then there is a natural choice for the shape of confidence intervals. For the observed data set ($D_{(0)}$, the value $\chi^2$ is a minimum at $a_{(0)}$. This chi-square may be called as $\chi^2_{min}$. If the vector **a** of the parameter values is perturbed away from $a_{(0)}$, then $\chi^2$ increases. The region within which $\chi^2$ increases by no more than a set amount $\Delta\chi^2$ defines some M dimensional confidence region around $a_{(0)}$. If $\Delta\chi^2$ is set to be a large number, this will be a big region, and it will be small region for small number. Some where in between there will be a choice of $\Delta\chi^2$ which will cause the region to contain variously, 68 percent, 90 percent, etc. of probability distribution for a's (parameters set). These regions are taken as the confidence regions for the parameters $a_{(0)}$. Fig. C.1 and C.2 shows two dimensional (M=2) confidence regions corresponding to several values of $\Delta\chi^2$. The one-dimensional confidence interval in $a_2$ corresponding to the region bounded by $\Delta\chi^2 = 1$ lies between the lines A and A'.

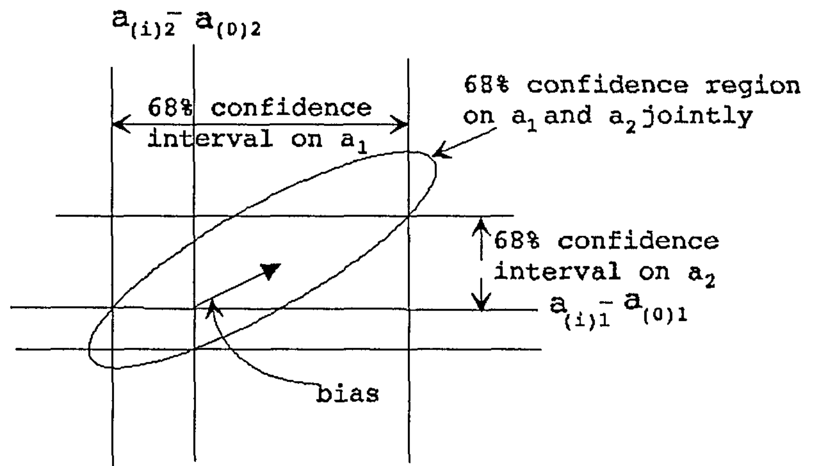


Fig. C.1 Confidence intervals in 1 and 2 dimensions

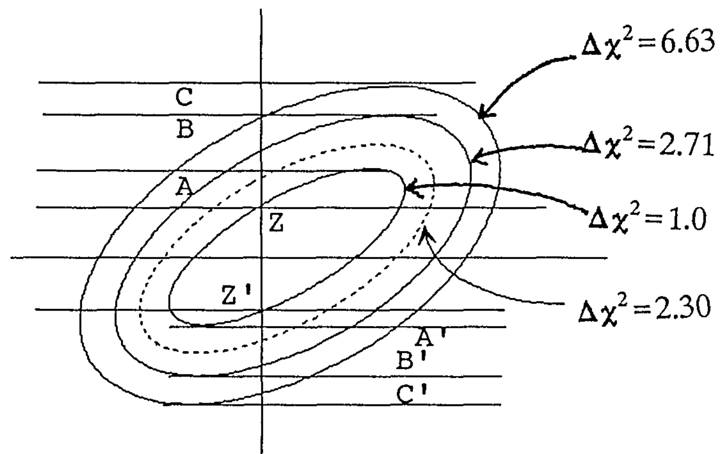


Fig. C.2 Confidence region ellipses corresponding to values of chi-square larger than the fitted minimum.

It may be noted that the projection of higher-dimensional region on the lower dimension space is used, not the intersection. The intersection would be the band between Z and Z' and it is never used.

$\Delta\chi^2$ as a function of confidence level and degree of freedom

| p(probability) | degrees of freedom |
|---|---|
| 68.3% of time | 2.3 ($\Delta\chi^2$) |
| 95.4% of time | 6.17 ($\Delta\chi^2$) |
| 99.73% of time | 11.8 ($\Delta\chi^2$) |

Therefore, the dashed ellipse ($\Delta\chi^2$ =2.30), contains 68.3 percent of the probability distribution, is a confidence region for $a_1$ and $a_2$ jointly, at this level of confidence.

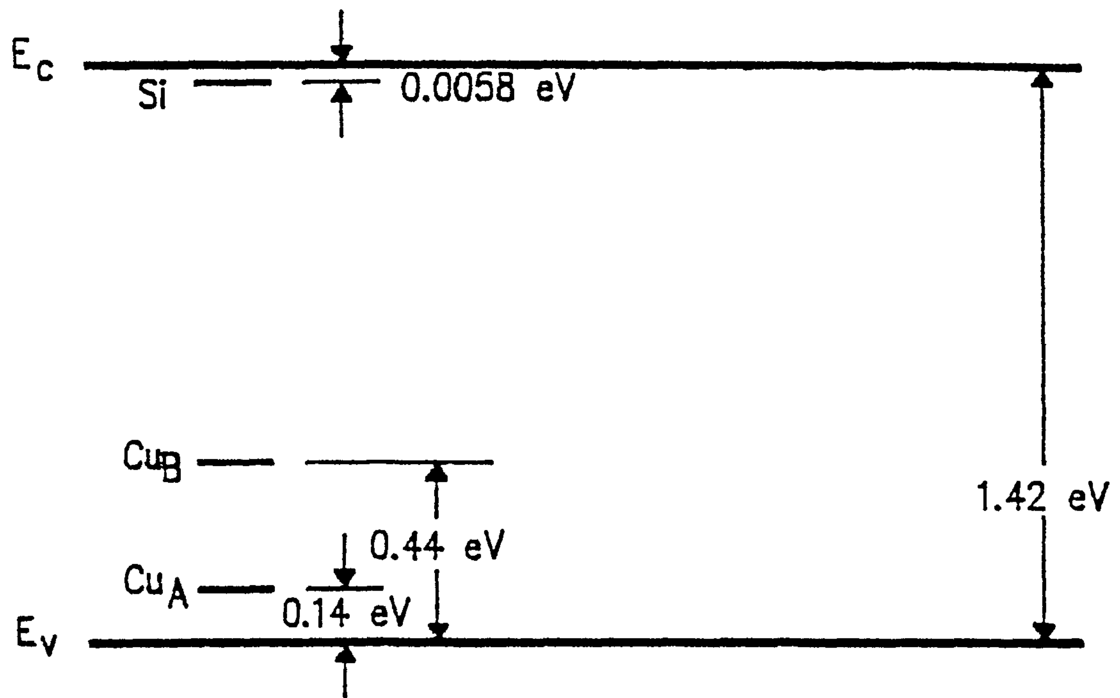


Fig. C.3 Energy level diagram of GaAs:Si:Cu at 300K [12].

# FLOW CHART

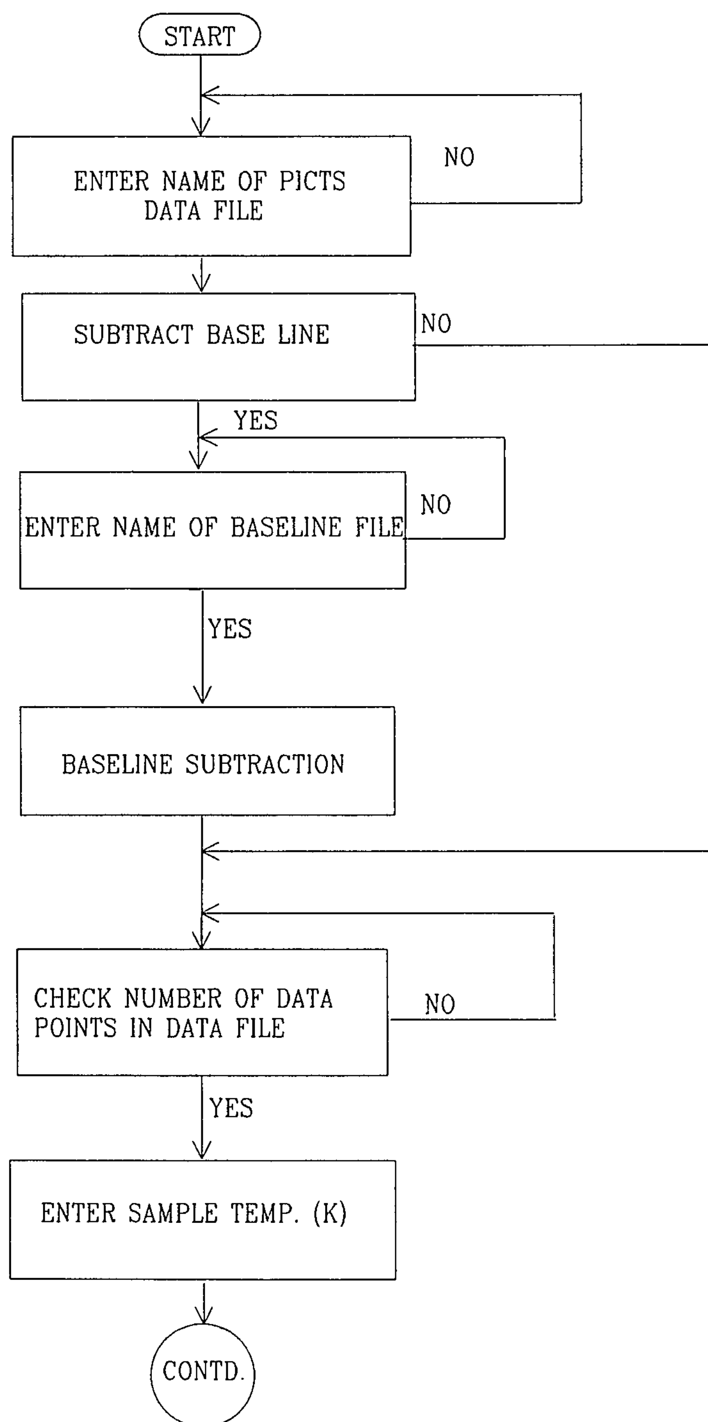

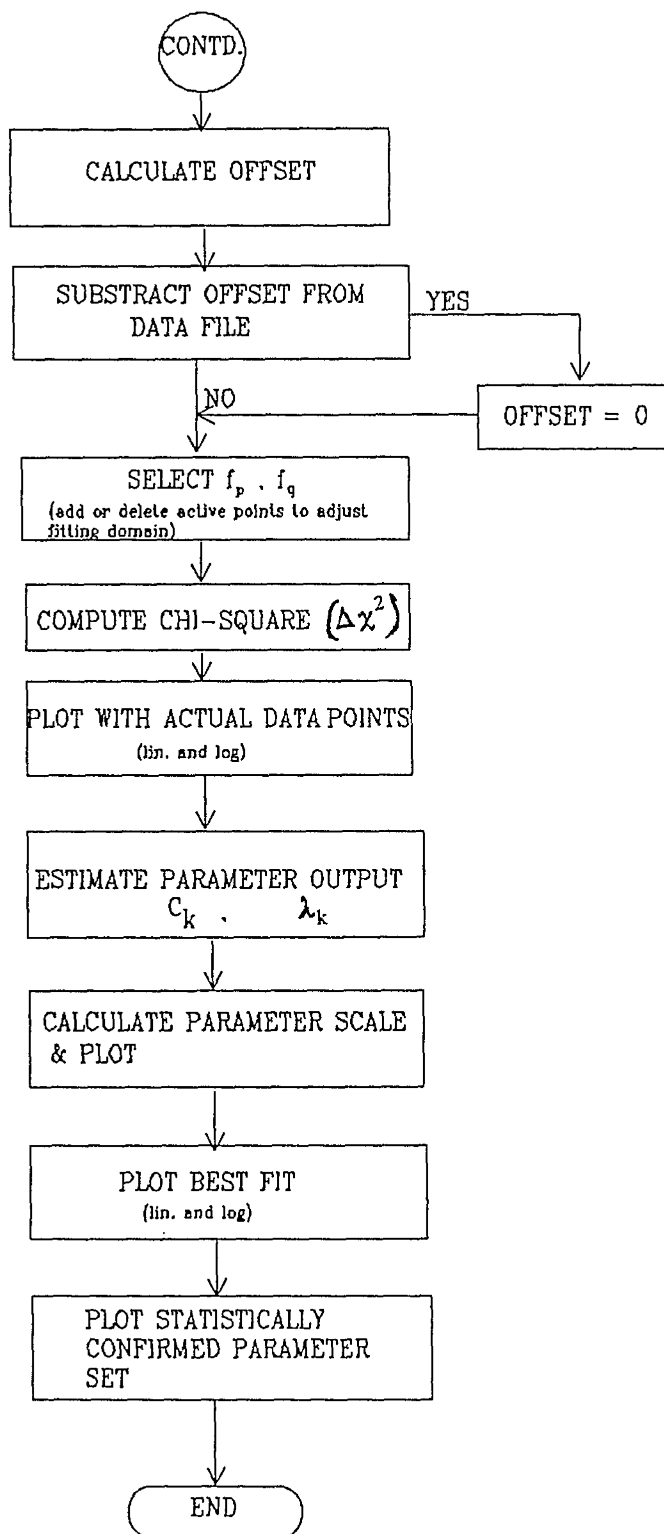
CONTD.
CALCULATE OFFSET
SUBSTRACT OFFSET FROM DATA FILE
YES
OFFSET = 0
NO
SELECT $f_p$ , $f_q$
(add or delete active points to adjust fitting domain)
COMPUTE CHI-SQUARE $(\Delta\chi^2)$
PLOT WITH ACTUAL DATA POINTS
(lin. and log)
ESTIMATE PARAMETER OUTPUT
$C_k$ , $\lambda_k$
CALCULATE PARAMETER SCALE & PLOT
PLOT BEST FIT
(lin. and log)
PLOT STATISTICALLY CONFIRMED PARAMETER SET
END

Evaluation of the digitizer data file uv70.wav at temperature T = 121.6 K.
Total Number of data points: 1023. Number of actual used data points: 871.
Window of best resolution: 1.175E+01 s-1 < lambda < 1.023E+04 s-1
Conservative estimate gives 3 exponential modes with chi**2 = 6.257E+03.
The corresponding parameters are statistically significant, however note that the errors may be underestimated due to a non-Gaussian distribution.

| Mode | Amplitude [Vs] | Decay-Constant [s-1] |
|---|---|---|
| 1 | 8.075E-03 +- 4.731E-05 | 2.042E+02 +- 1.764E+00 |
| 2 | 7.064E-04 +- 2.504E-05 | 1.068E+03 +- 2.414E+01 |
| 3 | 5.489E-02 +- 5.194E-05 | 3.505E+01 +- 6.246E-02 |

Higher order estimate gives 4 exponential modes with chi**2 = 4.815E+03.
The corresponding parameters are statistically not significant, but compare:

| Mode | Amplitude [Vs] | Time-Constant [s-1] |
|---|---|---|
| 1 | 1.487E-02 +- 9.825E-04 | 1.193E+02 +- 4.108E+00 |
| 2 | 1.797E-03 +- 5.408E-05 | 6.540E+02 +- 1.060E+01 |
| 3 | 7.277E-02 +- 2.938E-02 | 2.095E+01 +- 4.936E+00 |
| 4 | -1.109E+00 +- 6.550E+01 | 1.751E-01 +- 1.064E+01 |

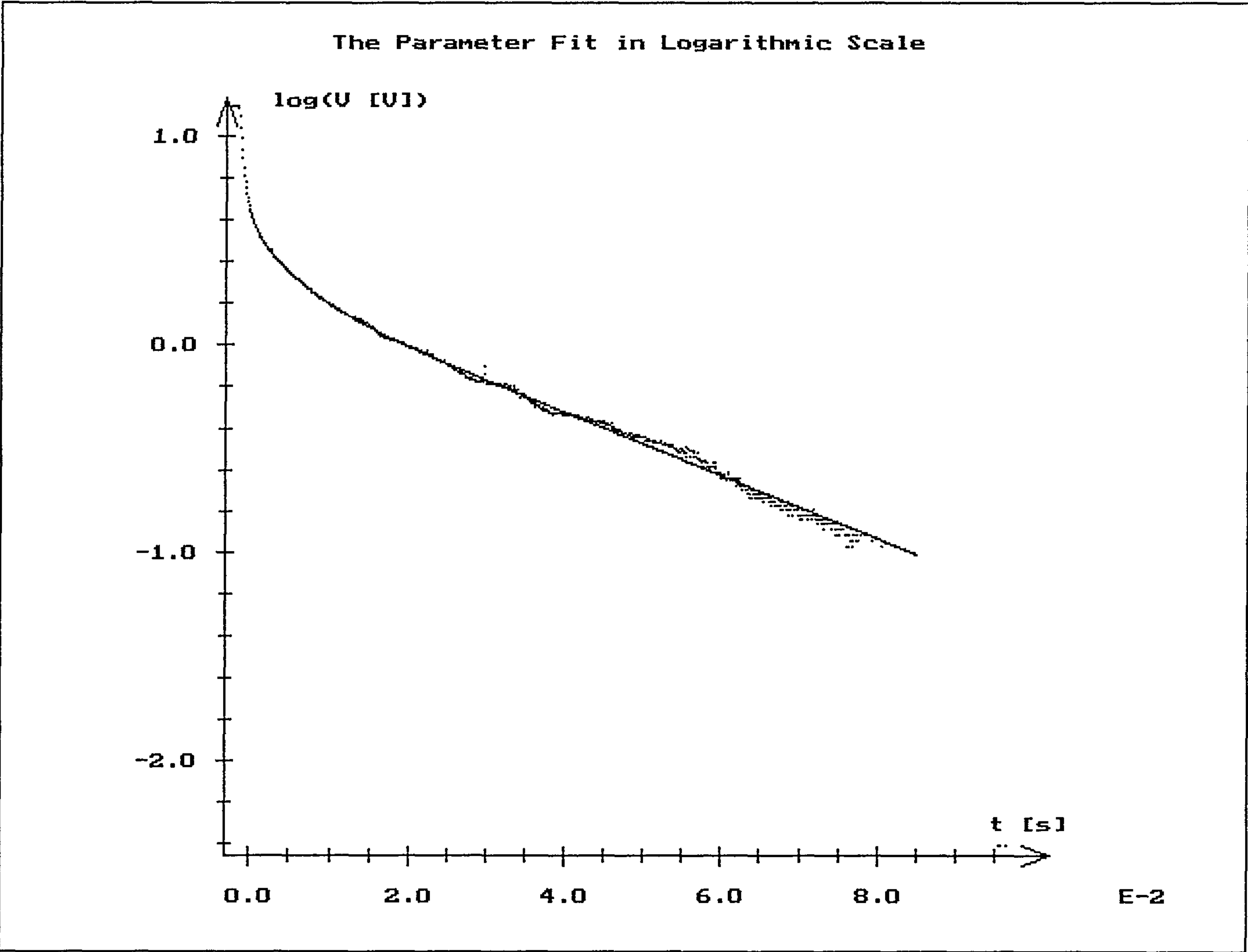
The Parameter Fit in Logarithmic Scale
log(V [V])
1.0
0.0
-1.0
-2.0
t [s]
0.0
2.0
4.0
6.0
8.0
E-2

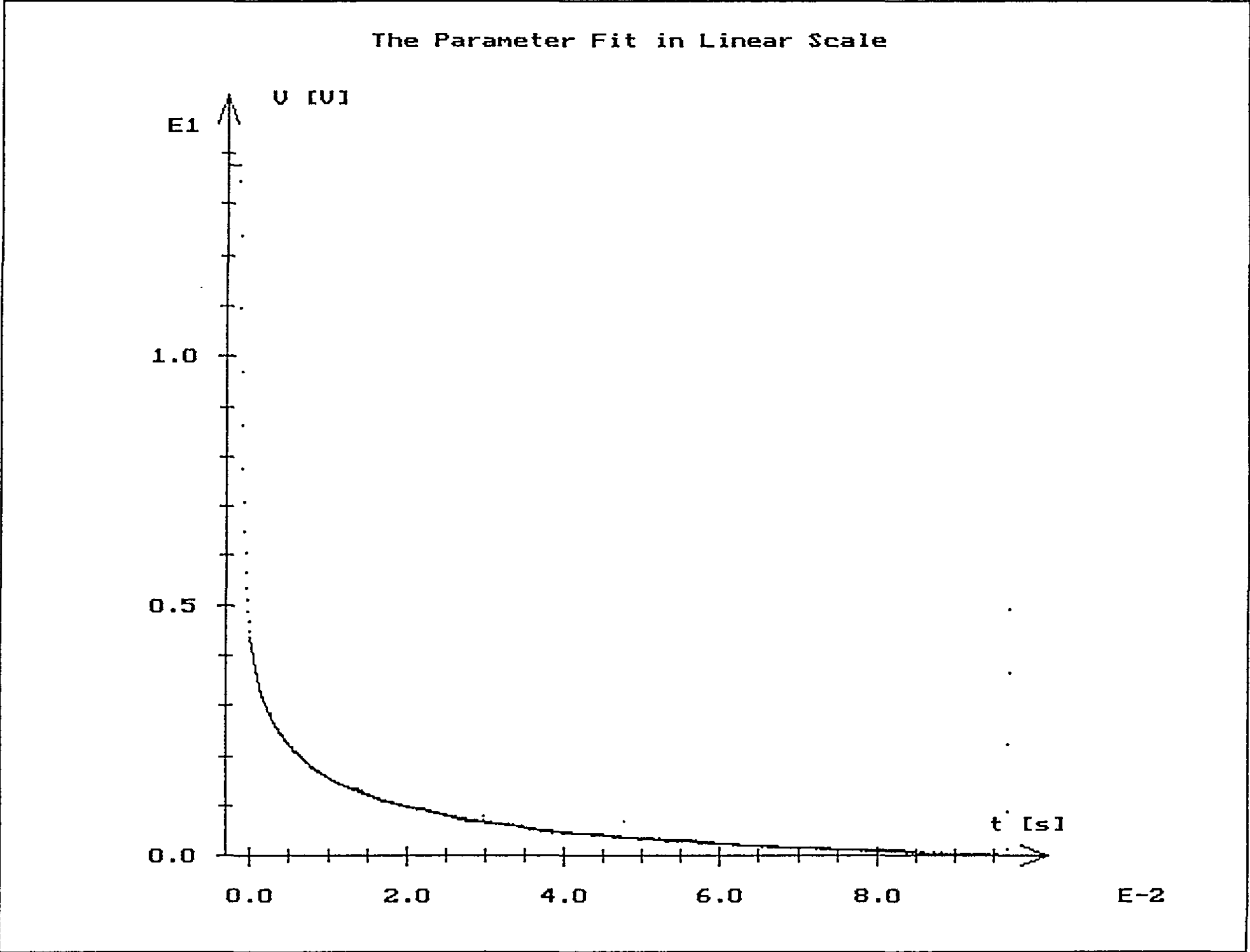

The Parameter Fit in Linear Scale
V [V]
E1
1.0
0.5
0.0
t [s]
0.0
2.0
4.0
6.0
8.0
E-2

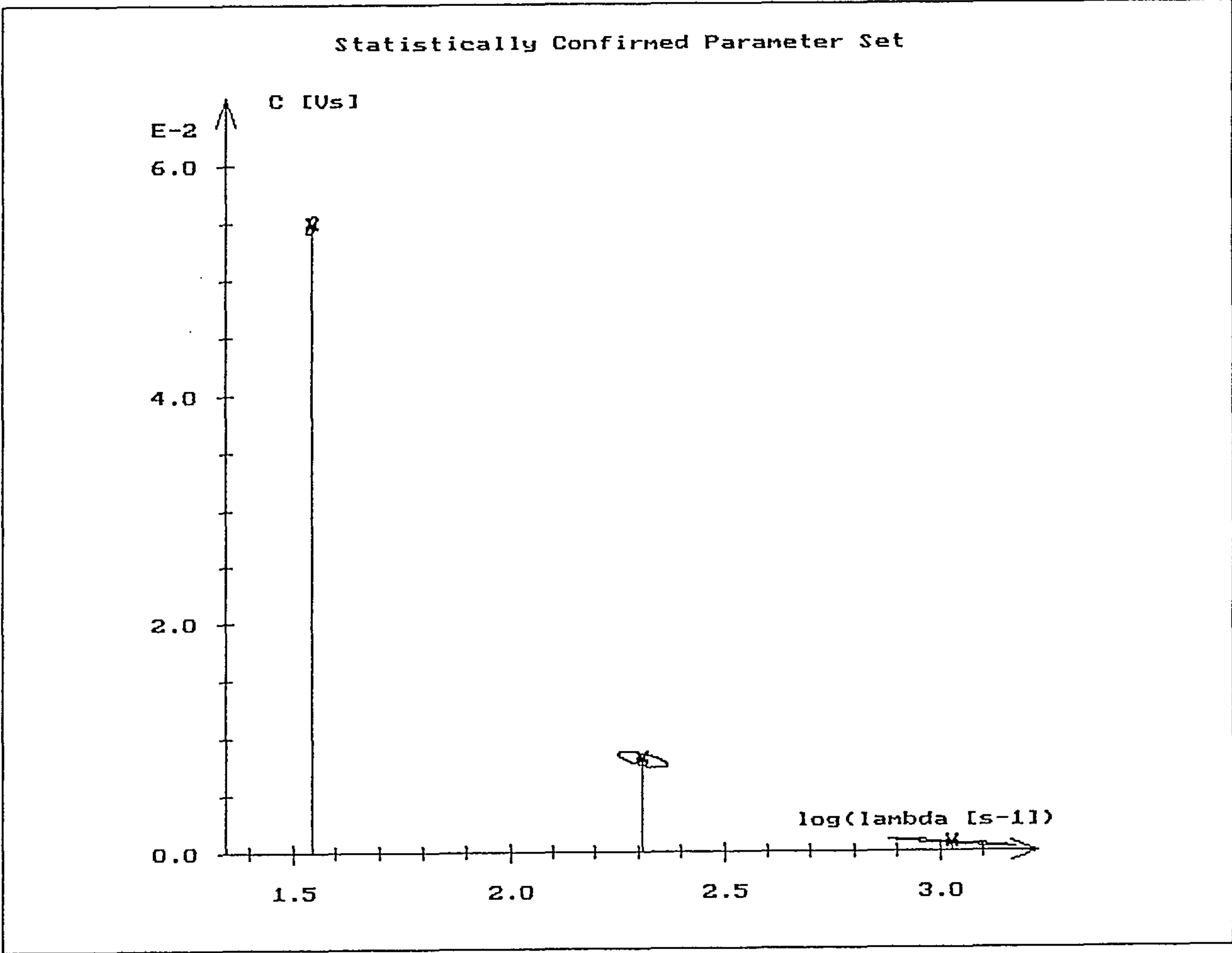
Statistically Confirmed Parameter Set
C [Vs]
E-2
6.0
4.0
2.0
0.0
1.5
2.0
2.5
3.0
log(lambda [s-1])

## APPENDIX-D

```
Program PICTS_Data_Analyzing_Program;
(***********************************************************************)
(*                                                                     *)
(*  This is a program to estimate the parameters of a PICTS signal using a    *)
(*  least-square parameter fit. Statistical tests (chi**2) are performed.     *)
(*                                                                     *)
(*                       M                                             *)
(*  Model:          i(t) = Σ   C_k μ_k exp(-μ_k*t)                      *)
(*                        k=1                                          *)
(*                                                                     *)
(*  Sampling:       i_k = i(k*T),   1 <= k <= npt                       *)
(*                                                                     *)
(*  The name of the data-file FileName is asked from the user, the number     *)
(*  npt of data points has to be specified in the CONST section (line 29).    *)
(*                                                                     *)
(*                                                                     *)
(*  Version:    July, 1992, with baseline subtraction included.        *)
(*                                                                     *)
(***********************************************************************)

{$M 65520, 0, 655360}
{$N+}   (* Use the '87 numeric co-processor, essentially to avoid overflow     *)
{$E+}
{$R+}   (* Range checking on                                           *)
{$D+}   (* Debug information                                           *)
{$L+}   (*                                                             *)

USES Crt,Shutdown,Dialogue,Functs,Graph,ColorDef,PlotM, Linsvmod, GeometrM;

CONST npt=1023;                     {Up to 4096 points are possible}

TYPE DigitData = ARRAY [1..npt] OF integer;

TYPE DataSet = RECORD
            Temperature,VoltageStep,TimeStep: extended;
            y : DigitData;
            OffSet : extended;
            Maxxy,Minny,fp,fq: integer;
            DName : string;
          END;

TYPE DataFormat = RECORD
              DataPoints : integer;
              DtFileName : string;
              VoltageDiv : real;
              TimeDiv    : real;
              CreatTime  : string;
              CreatDate  : string
            END;

PROCEDURE DecodeFormat(FormatLine:String;VAR Format:DataFormat);
VAR dum : string;
```

```
    kpos,code: integer;
BEGIN
    WITH Format DO
    BEGIN
        kpos := Pos(',',FormatLine);
        dum := copy(FormatLine,1,kpos-1);
        delete(FormatLine,1,kpos+1);
        Val(dum,DataPoints,code);
        IF code<>0 THEN
            ErrorStop('Format conversion error!');
        DataPoints := DataPoints+1;
        kpos := Pos('"',FormatLine);
        DtFileName := copy(FormatLine,1,kpos-1);
        delete(FormatLine,1,kpos+8);
        kpos := Pos(';',FormatLine);
        dum := copy(FormatLine,1,kpos-1);
        delete(FormatLine,1,kpos+3);
        Val(dum,VoltageDiv,code);
        IF code<>0 THEN
            ErrorStop('Format conversion error!');
        kpos := Pos(';',FormatLine);
        dum := copy(FormatLine,1,kpos-1);
        delete(FormatLine,1,kpos+3);
        Val(dum,TimeDiv,code);
        IF code<>0 THEN
            ErrorStop('Format conversion error!');
        kpos := Pos('"',FormatLine);
        CreatTime := copy(FormatLine,1,kpos-1);
        delete(FormatLine,1,kpos+2);
        kpos := Pos('"',FormatLine);
        CreatDate := copy(FormatLine,1,kpos-1);
    END
END;

FUNCTION NameMatched(FN1,FN2:string): boolean;
VAR result:boolean;
    k : integer;
BEGIN
    WHILE Pos(' ',FN1)>0 DO
        delete(FN1,1,1);
    WHILE Copy(FN1,Length(FN1),1) = ' ' DO
        delete(FN1,Length(FN1),1);
    WHILE Pos(' ',FN2)>0 DO
        delete(FN2,1,1);
    WHILE Copy(FN2,Length(FN2),1) = ' ' DO
        delete(FN2,Length(FN2),1);
    result := (Length(FN1) = Length(FN2));
    IF result=TRUE THEN
        FOR k:=1 TO Length(FN1) DO
            result := result AND (UpCase(FN1[k])=UpCase(FN2[k]));
    NameMatched := result
END;

PROCEDURE ReadDataFromFile(VAR ActData: DataSet);
VAR i,IOCode:integer;
VAR Diff,Diffmax,yalt,DFyi,BLFyi:integer;
    DataFile,BaseLineFile:text;
    DataFormatLine,BaseLineFormatLine,FileName,BaseLineName:string;
    ActDataFormat,BaseLineFormat:DataFormat;
    BaseLineSubtract: boolean;
BEGIN
    ClrScr;
```

```
gotoXY(1,1);
writeln('Welcome to the world of RP Brinkmann''s PICTS program with ',
npt:4,' data points!');
writeln('Input is a file of digitizer data describing the decay of laser induced ');
writeln;
writeln('Output are the inverse time constants of the current decay, the amplitudes');
writeln('of the corresponding normal modes, and error estimates for all quantities.');
writeln;
{$I-}
REPEAT
   write('Enter the name of the PICTS data file: ');
   readln(FileName);
   assign(DataFile,FileName);
   reset(DataFile);
   IOCode := IOResult;
   IF IOCode<>0 THEN
      writeln('Data file "',FileName,'" does not exist. Try again!')
UNTIL IOCode = 0;
writeln;
write('Substract a baseline file (y/n)?');
BaseLineSubtract := (Upcase(readkey) = 'Y');
IF BaseLineSubtract THEN
REPEAT
   writeln;
   write('Enter the name of the PICTS baseline file: ');
   readln(BaseLineName);
   assign(BaseLineFile,BaseLineName);
   reset(BaseLineFile);
   IOCode := IOResult;
   IF IOCode<>0 THEN
      writeln('Data file "',BaseLineName,'" does not exist. Try again!')
UNTIL IOCode = 0;
writeln;
REPEAT
   write('Enter the temperature of the sample in Kelvin: ');
   readln(ActData.Temperature);
   IOCode := IOResult;
   IF IOCode<>0 THEN
      writeln('Please correct the temperature input!')
UNTIL IOCode = 0;
{$I+}
readln(DataFile,DataFormatLine);
DecodeFormat(DataFormatLine,ActDataFormat);
IF NOT NameMatched(ActDataFormat.DtFileName,FileName) THEN
BEGIN
   writeln('Warning: Name of digitizer data file is not matched!');
   writeln('Compare ',ActDataFormat.DtFileName,' and ',FileName);
   WaitForUserToHitReturn;
END;
IF BaseLineSubtract THEN
BEGIN
   readln(BaseLineFile,BaseLineFormatLine);
   DecodeFormat(BaseLineFormatLine,BaseLineFormat);
   IF NOT NameMatched(BaseLineFormat.DtFileName,BaseLineName) THEN
   BEGIN
      writeln('Warning: Name of digitizer baseline file is not matched!');
      writeln('Compare ',BaseLineFormat.DtFileName,' and ',BaseLineName);
      WaitForUserToHitReturn;
   END;
   IF ActDataFormat.DataPoints<>BaseLineFormat.DataPoints THEN
      ErrorStop('Numbers of data and baseline points do not match!');
END;
```

```
  IF ActDataFormat.DataPoints< >npt THEN
    ErrorStop('Number of data points in CONST section must be changed!');
  ClrScr;
  WITH ActData DO
  BEGIN
    DName := FileName;
    writeln;
    writeln('Temperature of the environment: ', Temperature:6:2,' K');
    VoltageStep := ActDataFormat.VoltageDiv/128;
    write('Voltage per digitizer step: ');
    putreal(VoltageStep); writeln(' V');
    TimeStep := ActDataFormat.TimeDiv*10/1023;
    write('Timestep between two samplings: ');
    putreal(TimeStep); writeln(' s');
    yalt := -10000;
    Diffmax := 10000;
    Maxxy := -10000;
    Minny := 10000;
    FOR i := 1 to npt DO
    BEGIN
      readln(DataFile,DFyi);
      IF BaseLineSubtract THEN
      BEGIN
        readln(BaseLineFile,BLFyi);
        y[i] := DFyi-BLFyi;
      END
      ELSE
        y[i] := DFyi;
      IF y[i]>Maxxy THEN
         Maxxy := y[i];
      IF y[i]<Minny THEN
         Minny := y[i];
      IF (y[i]-yalt<Diffmax) AND (y[i]-yalt<0) THEN
      BEGIN
        Diffmax := y[i]-yalt;
        fp := i-1
      END;
      yalt := y[i]
    END;
    IF fp<1 THEN fp:=1;
    fq := npt;
    OffSet := Minny-0.5;
    writeln;
    write('The offset is = ');
    putreal(OffSet);
    writeln;
    write('Substract the offset from the data (y/n)?');
    IF (Upcase(readkey) = 'Y') THEN
      OffSet := 0;
  END;
  close(DataFile);
  IF BaseLineSubtract THEN
    close(BaseLineFile);
END;

TYPE ScaleMode = (Linear,Logarithmic);

PROCEDURE SetDataScale(tMin,tMax,MinVolt,MaxVolt:extended;
                Headline:string; ScaleMod:ScaleMode);
BEGIN
  pen(schwarz);
  box;
```

```
   IF ScaleMod = Linear THEN
   BEGIN
      scale(1.05*Tmin,1.05*Tmax,0.0,1.1*MaxVolt,Space);
      Coordinates(LeftAndBelow,Headline,'t [s]','V [V]');
   END
   ELSE
   BEGIN
      scale(1.05*Tmin,1.05*Tmax,log(0.9*MinVolt),log(1.1*MaxVolt),Space);
      Coordinates(LeftandBelow,Headline,'t [s]','log(V [V])');
   END
END;

PROCEDURE CalculateParameterScale(VAR lmin,lmax,Cmax: extended; a: Vector;
                                  Modes: integer; VoltageScale: extended);
VAR k : integer;
BEGIN
   lmin := 1.0E+1000;
   lmax :=-1.0E+1000;
   Cmax :=-1.0E+1000;
   FOR k:=1 TO Modes DO
   BEGIN
      IF a[2*k-1]>lmax THEN
         lmax := a[2*k-1];
      IF a[2*k-1]<lmin THEN
         lmin := a[2*k-1];
      IF a[2*k-2]>Cmax THEN
         Cmax := a[2*k-2]*VoltageScale;
   END;
END;

PROCEDURE SetParameterScale(lmin,lmax,Cmax:extended; Headline:string);
BEGIN
   pen(schwarz);
   scale(log(lmin)-0.2,log(lmax)+0.2,0.0,1.2*Cmax,Space);
   box;
   Coordinates(Leftandbelow,Headline,'log(lambda [s-1])','C [Vs]');
END;

PROCEDURE PlotDataPoints(ScaleMod:ScaleMode; ActData: DataSet);
VAR k:integer;
BEGIN
   WITH ActData DO
      IF ScaleMod = Linear THEN
      BEGIN
         pen(hellblau);
         FOR k:=1 TO fp-1 DO
            pointsymbol((k-fp)*TimeStep,(y[k]-Offset)*VoltageStep,Point);
         pen(hellrot);
         FOR k:=fp TO fq DO
            pointsymbol((k-fp)*TimeStep,(y[k]-OffSet)*VoltageStep,Point);
         pen(hellblau);
         FOR k:=fq+1 TO npt DO
            pointsymbol((k-fp)*TimeStep,(y[k]-OffSet)*VoltageStep,Point);
      END
      ELSE IF ScaleMod = Logarithmic THEN
      BEGIN
         pen(hellblau);
         FOR k:=1 TO fp-1 DO
            pointsymbol((k-fp)*TimeStep,log((y[k]-OffSet)*VoltageStep),Point);
         pen(hellrot);
         FOR k:=fp TO fq DO
            pointsymbol((k-fp)*TimeStep,log((y[k]-OffSet)*VoltageStep),Point);
```

```
        pen(hellblau);
        FOR k:=fq+1 TO npt DO
          pointsymbol((k-fp)*TimeStep,log((y[k]-OffSet)*VoltageStep),Point);
      END
END;


PROCEDURE funcs(ii,iiOffset: integer; TimeScale: extended; a: Vector;
          VAR y: extended; VAR dyda: Vector; Modes: integer);
VAR
  k,tkm2,tkm1 : integer;
  dum,dim:extended;
BEGIN
  y := 0;
  FOR k := 1 to Modes DO
  BEGIN
     tkm1 := k+k-1;
     tkm2 := tkm1-1;
     dum := a[tkm1]*(ii-iiOffset)*TimeScale;
     dim := uxp(-dum);
     dyda[tkm2] := a[tkm1]*dim;
     dyda[tkm1] := a[tkm2]*(1-dum)*dim;
     y := y + a[tkm2]*dyda[tkm2];
  END;
END;

FUNCTION FitVal(Modes: integer; t:extended; a:Vector): extended;
VAR
  k : integer;
  sum,dum:extended;
BEGIN
  sum := 0;
  FOR k := 1 to Modes DO
  BEGIN
     dum := a[2*k-1]*t;
     sum := sum + a[2*k-2]*a[2*k-1]*uxp(-dum)
  END;
  FitVal := sum;
END;


PROCEDURE PlotBestFit(Modes: integer; TimeScale,VoltScale: extended;
              ScaleMod: ScaleMode; a:Vector; fp,fq:integer);
VAR k: integer;
   t: extended;
BEGIN
   pen(hellgruen);
   IF ScaleMod = Linear THEN
   BEGIN
      t := 0;
      jump(t,VoltScale*FitVal(Modes,t,a));
      FOR k:=1 TO fq-fp DO
      BEGIN
         t := t + TimeScale;
         draw(t,VoltScale*Fitval(Modes,t,a))
      END
   END
   ELSE IF ScaleMod = Logarithmic THEN
   BEGIN
      t := 0;
      jump(t,log(VoltScale*FitVal(Modes,t,a)));
      FOR k:=1 TO fq-fp DO
```

```
      BEGIN
        t := t + TimeScale;
        draw(t,log(VoltScale*Fitval(Modes,t,a)))
      END
    END;
END;

 VAR
    chisq,chisqnew,glochisq: extended;
    covar,covarnew : matrix;
    a,anew,glbeta : Vector;
    k   : integer;

PROCEDURE mrqcof(TimeScale:extended; y: DigitData; OffSet:extended; fp,fq: integer;
              VAR a: Vector; VAR alpha: Matrix;
              VAR beta: Vector; VAR chisq: extended; Modes:integer);
VAR
    k,j,i: integer;
    ymod,wt,dy: extended;
    dyda: Vector;
BEGIN
    FOR j := 0 to P DO
    BEGIN
      FOR k := 0 to j DO
        alpha[j,k] := 0.0;
      beta[j] := 0.0
    END;
    chisq := 0.0;
    FOR i := fp to fq DO
    BEGIN
      funcs(i,fp,TimeScale,a,ymod,dyda,Modes);
      dy := y[i]-OffSet-ymod;
      FOR j := 0 to P DO
      BEGIN
        wt := dyda[j];
        FOR k := 0 to j DO
          alpha[j,k] := alpha[j,k]+wt*dyda[k];
        beta[j] := beta[j]+dy*wt
      END;
      chisq := chisq+dy*dy
    END;
    FOR j := 1 to P DO
      FOR k := 0 to j-1 DO
        alpha[k,j] := alpha[j,k]
END;


PROCEDURE mrqmin(TimeScale:extended;y: DigitData; OffSet:extended;
              fp,fq:integer; VAR a: Vector;
              VAR covar,alpha: Matrix; VAR chisq,alamda : extended;
              VAR warte: integer; Modes:integer);
VAR
     i,j,k: integer;  xxx,atry,da: Vector;
     aa :Matrix;  indx:glindx;
     d:extended;
BEGIN
    IF (alamda < 0.0) THEN
    BEGIN
      warte := 0;
      alamda := 1.0E5;
      mrqcof(TimeScale,y,Offset,fp,fq,a,alpha,glbeta,chisq,Modes);
      glochisq := chisq;
```

```
      atry := a;
   END;
   covar := alpha;
   FOR j := 0 TO P DO
      covar[j,j] :=alpha[j,j]*(1.0+alamda);
   aa := covar;
   xxx := glbeta;
   ludcmp(aa,indx,d);
   lubksb(aa,indx,xxx);
   mprove(covar,aa,indx,glbeta,xxx);
   FOR j:=0 TO P DO
   BEGIN
      FOR i:=0 TO P DO da[i]:=0;
      da[j] := 1;
      lubksb(aa,indx,da);
      FOR i:=0 TO P DO covar[i,j]:=da[i]
   END;
      da := xxx;
      IF NOT (alamda = 0.0) THEN
      BEGIN
         FOR j := 0 TO P DO
            atry[j] := a[j]+da[j];
         mrqcof(TimeScale,y,OffSet,fp,fq,atry,covar,da,chisq,Modes);
         IF (chisq < glochisq) THEN
         BEGIN
            IF warte< =0 THEN
               alamda := 0.5*alamda;
            IF warte<-2 THEN
               alamda := 0.4*alamda;
            warte := warte-1;
            glochisq := chisq;
            alpha := covar;
            glbeta := da;
            a := atry
         END
         ELSE
         BEGIN
            alamda := 2*alamda;
            warte := 5;
            chisq := glochisq
         END;
      END
END;

PROCEDURE LocalMinimum(ActData:DataSet; VAR a:Vector; VAR chisq:extended;
               VAR covar:Matrix; Modes:integer);
VAR warte,itst,kl: integer;
   alamda,oldchisq,ochisq :extended;
   alpha : Matrix;
BEGIN
   gotoXY(1,1);
   write('Modes Steps   chi**2    D_chi**2   Converge   wait   alamda    itst');
   oldchisq := chisq;
   alamda := -1;
   WITH actdata DO
      mrqmin(timestep,y,Offset,fp,fq,a,covar,alpha,chisq,alamda,warte,Modes);
   ochisq := chisq;
   kl := 1;
   itst := 0;
   While   ((oldchisq-chisq> 1) AND ((itst< =50) OR (kl<100)))
       OR ((oldchisq-chisq< =1) AND (kl<1000)) DO
   BEGIN
```

```
      gotoXY(1,3);
      write(Modes:4);
      write(kl  :7);
      write('  '); putreal(chisq);        write(' ');
      write(' '); putreal(oldchisq-chisq); write(' ');
      write(' '); putreal(ochisq-chisq); write(' ');
      write(warte:6);
      write('  '); putreal(alamda);       write(' ');
      write(itst:6);
      kl := kl+1;
      ochisq := chisq;
      WITH actdata DO
         mrqmin(timestep,y,offset,fp,fq,a,covar,alpha,chisq,alamda,warte,Modes);
      IF alamda>1.0E20 THEN
         kl := kl+10;
      IF (ochisq-chisq > 0.002) THEN
         itst := 0
      ELSE
         itst := itst+1;
   END;
   alamda := 0.0;
   WITH actdata DO
       mrqmin(timestep,y,offset,fp,fq,a,covar,alpha,chisq,alamda,warte,Modes);
   ClrScr;
END;

FUNCTION PairAcceptable(C,lambda,VarC,Varlambda:extended):boolean;
BEGIN
   PairAcceptable := (C/VarC>2) AND (lambda>0) AND (lambda/Varlambda>2)
END;

FUNCTION SetAcceptable(a:Vector;covar:Matrix; Modes:integer):boolean;
VAR k:integer;
   res:boolean;
BEGIN
   res := TRUE;
   FOR k:=1 TO Modes DO
      res := res AND (covar[2*k-2,2*k-2]>0) AND (covar[2*k-1,2*k-1]>0)
              AND  PairAcceptable(a[2*k-2],a[2*k-1],
                 sqrt(covar[2*k-2,2*k-2]),sqrt(covar[2*k-1,2*k-1]));
   SetAcceptable := res;
END;


PROCEDURE ParameterOutput(actdata:DataSet; a,anew:Vector; chisq,chisqnew:extended;
                    covar,covarnew:Matrix;
                    Modes:integer; hidden: boolean);
VAR k1,k2:integer;
BEGIN
   WITH ActData DO
   BEGIN
      ClrScr;
      writeln;
      writeln('Evaluation of the digitizer data file ',DName,
            ' at temperature T = ',Temperature:5:1,' K.');
      writeln('Total Number of data points: ',npt:3,'.',
            '  Number of actual used data points: ',
                        fq-fp+1:3,'.');
      write('Window of best resolution: ');
      putreal(1/((fq-fp+1)*TimeStep));
      write(' s-1  < lambda < ');
      putreal(1/TimeStep);
```

```
      writeln(' s-1 ');
      write('Conservative estimate gives',Modes:3,' exponential modes ',
            'with chi**2 ='); putreal(chisq); writeln('. ');
      writeln('The corresponding parameters are statistically significant, however note');
      writeln('that the errors may be underestimated due to a non-Gaussian distribution.');
      writeln;
      writeln('Mode      Amplitude [Vs]        Decay-Constant [s-1]');
      FOR k:=1 TO Modes DO
      BEGIN
        k2 := 2*k-2;
        k1 := k2+1;
        writeln;
        write(k:3,'  ');;
        putreal(a[k2]*ActData.VoltageStep);
        write(' +-');
        putreal(sqrt(covar[k2,k2])*ActData.VoltageStep);
        write('  ');
        putreal(a[k1]);
        write(' +-');
        putreal(sqrt(covar[k1,k1]));
        write('    ');
      END;
      writeln;
      writeln;
      IF hidden THEN
      BEGIN
        write('Higher order estimate gives',Modes+1:3,' exponential modes ',
              'with chi**2 ='); putreal(chisqnew); writeln('. ');
        writeln('The corresponding parameters are statistically not significant, but compare:');
        writeln;
        writeln('Mode      Amplitude [Vs]        Time-Constant [s-1]');
        FOR k:=1 TO Modes+1 DO
        BEGIN
          k2 := 2*k-2;
          k1 := k2+1;
          writeln;
          write(k:3,'  ');;
          putreal(anew[k2]*ActData.VoltageStep);
          write(' +-');
          IF covarnew[k2,k2]>0 THEN
            putreal(sqrt(covarnew[k2,k2])*ActData.VoltageStep)
          ELSE
            write(' undefined');
          write('  ');
          putreal(anew[k1]);
          write(' +-');
          IF covarnew[k1,k1]>0 THEN
            putreal(sqrt(covarnew[k1,k1]))
          ELSE
            write(' undefined');
          write('    ');
        END;
      END;
    END
  END;

PROCEDURE DrawMode(X,Y,c11,c12,c21,c22,Lx,Ly:extended);
VAR C,A: TwoMat;
  xc : TwoVec;
  xs,Xln10: extended;
CONST Dchi2_1 =  2.30;  {68.30%}
      Dchi2_2 =  6.17;  {95.40%}
```

```
    Dchi2_3 = 11.80;  {99.73%}
    Dchi2_4 =230.00;  {Empirical form factor}
BEGIN
   Xln10 := X*ln(10);
   xs := log(X);
   jump(xs,0);
   drawchar(xs,Y,'X');
   SetMat(c11/sqr(Xln10),c12/Xln10,c21/Xln10,c22,C);
   InvMat(C,A);
   SetVec(xs,Y,xc);
   DrawEllipse(A,xc,Dchi2_1,Lx,Ly);
   DrawEllipse(A,xc,Dchi2_2,Lx,Ly);
   DrawEllipse(A,xc,Dchi2_3,Lx,Ly);
   DrawEllipse(A,xc,Dchi2_4,Lx,Ly);
END;


PROCEDURE Estimate(ActData: DataSet; VAR a,anew:Vector; VAR covar,covarnew:Matrix;
               VAR chisq,chisqnew,deltachi:extended;
               VAR Modes: integer; VAR hidden: boolean);
VAR EndCrit: boolean;
BEGIN
   Modes := 0;
   anew := a;
   covarnew := covar;
   chisqnew := chisq;
   EndCrit := FALSE;
   WHILE NOT EndCrit DO
   BEGIN
      a := anew;
      covar := covarnew;
      chisq := chisqnew;
      Modes := Modes + 1;
      P := 2*Modes-1;
      IF Modes = 1 THEN
      BEGIN
         anew[2*Modes-2] := ActData.VoltageStep;
         anew[2*Modes-1] := 0.2;
      END
      ELSE
      BEGIN
         anew[2*Modes-2] := 1.0E-5*ActData.VoltageStep;
         anew[2*Modes-1] := 0.1*anew[2*Modes-3]
      END;
      LocalMinimum(ActData,anew,chisqnew,covarnew,Modes);
      Endcrit := NOT SetAcceptable(anew,covarnew,Modes)
   END;
   Modes := Modes-1;
   P := 2*Modes-1;
   hidden := (chisq-chisqnew > 1.0);
   deltachi := chisq-chisqnew;
END;

VAR Imin,Imax,Cmax:extended;

VAR ActData: DataSet;

VAR dum,Deltachi: extended;
   hidden,EndCriterion: boolean;
   Modes:integer;
BEGIN
   ReadDataFromFile(ActData);
```

```
WITH ActData DO
BEGIN
  REPEAT
    writeln;
    writeln('In the following display, actually used data points are red, others are blue.');
    WaitForUserToHitReturn;
    InitPlot(ColorScreen,Laser);
    SetDataScale(-fp*TimeStep,(npt-fp)*TimeStep,
                 (Minny-Offset)*VoltageStep,
                 (Maxxy-Offset)*VoltageStep,
            'The Data Points in Linear Scale',linear);
    PlotDataPoints(Linear,ActData);
    next;
    SetDataScale(-fp*TimeStep,(npt-fp)*TimeStep,
                 (Minny-OffSet)*VoltageStep,
                 (Maxxy-Offset)*VoltageStep,
           'The Data Points in Logarithmic Scale',logarithmic);
    PlotDataPoints(Logarithmic,ActData);
    FinitPlot;
    writeln('You have the possibility to select a subset of data to be evaluated.');
    writeln;
    writeln('First active point fp: ',fp:4,
          ' Last active point fq: ',fq:4);
    writeln;
    write('Add or delete active points to adjust fitting domain (y/n)?');
    IF Upcase(readkey) = 'Y' THEN
    BEGIN
      EndCriterion := FALSE;
      writeln;
      writeln;
      write('Old first active point fp :',fp:4,' Give new fp: '); readln(fp);
      write('Old last active point fq  :',fq:4,' Give new fq: '); readln(fq);
    END
    ELSE
      EndCriterion := TRUE
  UNTIL EndCriterion;
  Clrscr;
  chisq := 1.0E+99;
  Estimate(ActData,a,anew,covar,covarnew,chisq,chisqnew,deltachi,Modes,hidden);
  ParameterOutput(ActData,a,anew,chisq,chisqnew,covar,covarnew,Modes,hidden);
  writeln;
  WaitForUserToHitReturn;
  InitPlot(ColorScreen,Laser);
  SetDataScale(-fp*TimeStep,(npt-fp)*TimeStep,
                 (Minny-Offset)*VoltageStep,
                 (Maxxy-Offset)*VoltageStep,
          'The Parameter Fit in Linear Scale',linear);
  PlotDataPoints(Linear,ActData);
  PlotBestFit(Modes,TimeStep,VoltageStep,Linear,a,fp,fq);
  next;
  SetDataScale(-fp*TimeStep,(npt-fp)*TimeStep,
                 (Minny-OffSet)*VoltageStep,
                 (Maxxy-OffSet)*VoltageStep,
          'The Parameter Fit in Logarithmic Scale',logarithmic);
  PlotDataPoints(Logarithmic,ActData);
  PlotBestFit(Modes,TimeStep,VoltageStep,Logarithmic,a,fp,fq);
  next;
  CalculateParameterScale(lmin,lmax,Cmax,a,Modes,VoltageStep);
  SetParameterScale(lmin,lmax,Cmax,
             'Statistically Confirmed Parameter Set');
  pen(hellrot);
  FOR k:=1 TO Modes DO
```

```
DrawMode(a[2*k-1],a[2*k-2]*VoltageStep,
        covar[2*k-1,2*k-1],covar[2*k-1,2*k-2]*VoltageStep,
        covar[2*k-2,2*k-1]*VoltageStep,
        covar[2*k-2,2*k-2]*VoltageStep*VoltageStep,
        log(Imax/Imin)+0.4,1.1*Cmax);
  FinitPlot;
 END
END.
```